marine drugs

MDPI

Review

Marine Natural Products in Ovarian Cancer Research: Mechanistic Evidence and Translational Priorities

Jing Jin [1], Yongyuan Wei [2,3,4], Dingmi Xiong [1], Siqi Liu [2,3,4], Ting Feng [2,3,4], Pei Wang [2,3,4], Liman Zhou [2,3,4,*], Renshuai Zhang [5,*] and Fandong Kong [1,2,3,4,*]

1 College of Ocean and Biology, Guangxi Minzu University, Nanning 530006, China; 19947830272@163.com (J.J.); xdm7026@163.com (D.X.)
2 Key Laboratory of Chemistry and Engineering of Forest Products, State Ethnic Affairs Commission, Guangxi Minzu University, Nanning 530006, China; 17300085996@163.com (Y.W.); 13781458574@163.com (S.L.); fengting124578@126.com (T.F.); wangpei850212@163.com (P.W.)
3 Guangxi Key Laboratory of Chemistry and Engineering of Forest Products, Guangxi Minzu University, Nanning 530006, China
4 Guangxi Collaborative Innovation Center for Chemistry and Engineering of Forest Products, Guangxi Minzu University, Nanning 530006, China
5 School of Pharmaceutical Sciences, Shandong First Medical University, Jinan 250117, China
* Correspondence: zhouliman88@126.com (L.Z.); rszhang@sdfmu.edu.cn (R.Z.); kongfandong0127@126.com (F.K.)

Abstract

Recurrence and treatment resistance continue to limit the long-term control of ovarian cancer. Marine natural products offer chemically diverse leads, but their development depends on evidence obtained in relevant disease models rather than on potency alone. This review examines representative compounds by biological source, chemical class, mechanism, and stage of development. Reported effects include apoptosis, cell-cycle arrest, inhibition of invasion and angiogenesis, ferroptosis-associated responses, and activity in drug-resistant models. We distinguish direct target engagement from downstream signaling changes and retained cytotoxicity from resensitization to chemotherapy. Examples such as Sec61 inhibition, distinct tubulin-binding modes, and ERK rescue experiments illustrate how different levels of evidence shape mechanistic interpretation. Recent studies of regulated cell death and tumor-associated macrophages are also discussed. Although animal data support several candidates, clinical experience with marine-derived agents shows that cellular activity does not necessarily translate into therapeutic benefit or acceptable tolerability. We therefore outline priorities for histotype-appropriate models, target validation, exposure-linked efficacy, sustainable production, and rigorous combination studies. These criteria provide a practical basis for selecting candidates without overstating the available preclinical evidence.

Keywords: ovarian cancer; marine natural products; target validation; chemoresistance; ferroptosis; drug discovery; clinical translation

Check for updates

Academic Editor: Sik Yoon

Received: 5 November 2026
Revised: 23 November 2026
Accepted: 24 November 2026
Published: 26 November 2026

Copyright: © 2026 by the authors. Licensee MDPI, Basel, Switzerland. This article is an open access article distributed under the terms and conditions of the Creative Commons Attribution (CC BY) license.

1. Introduction

Ovarian cancer is commonly diagnosed at an advanced stage and remains a major cause of cancer-related mortality. Population-based screening has not shown a mortality benefit in a large randomized trial [1,2]. Cytoreductive surgery followed by platinum–taxane chemotherapy is the standard first-line approach for most patients, but recurrence and acquired resistance are frequent [1]. Mechanisms of platinum resistance include enhanced DNA damage repair, altered drug transport, suppression of apoptosis, and phenotypic plasticity [3,4]. PARP inhibitor maintenance has improved progression-free survival in selected populations. SOLO1

demonstrated benefit in BRCA1/2-mutated disease, while PRIMA extended benefit beyond BRCA-mutated tumors, particularly in homologous-recombination-deficient disease [5,6]. Benefit is not uniform across molecular subgroups, and acquired resistance remains a limitation [7]. Pembrolizumab monotherapy had modest activity in recurrent ovarian cancer in KEYNOTE-100; tumor microenvironment studies further suggest that homologous recombination status and regulatory T cells influence treatment response [8,9]. Against this background, natural products continue to provide anticancer leads, with marine organisms representing a rich source of chemical diversity [10–13].

Marine natural products may include polycyclic frameworks, stereochemically complex macrocycles, halogenated metabolites, and peptide-derived scaffolds. This chemical diversity broadens the search for anticancer leads, although structural novelty alone says little about affinity, selectivity, or therapeutic value. In ovarian cancer models, these compounds affect proliferation, invasion, angiogenesis, and drug response. Interpretation of such findings depends on the experimental model, exposure conditions, and quality of mechanistic evidence; marine origin does not itself imply a shared pharmacological advantage [12–15].

We searched Web of Science, PubMed, Scopus, and CNKI to identify relevant studies for this narrative review. The search terms were: marine natural product, marine fungi, marine actinomycete, sponge, algae, ovarian cancer, cytotoxicity, anticancer activity. The search covered records from database inception through September 2026. Additional records were manually screened from the reference lists of included reviews and original articles to capture missed studies.

Here, we organize representative studies by biological source and then consider their mechanistic and translational implications. Table 1 summarizes the selected activity data, Figure 1 shows the publication years of the distinct reports cited in Table 1, and Figure 2 presents the corresponding numbered structures or preparations. The inventory is descriptive rather than systematic or bibliometric and is not intended to indicate temporal trends or discovery productivity. Throughout, we distinguish the organism from which a metabolite was isolated from its demonstrated biosynthetic producer and record the provenance of the material used in ovarian cancer assays. These distinctions matter particularly for sponge-associated metabolites and for fungal compounds tested using nonmarine or commercially sourced material [16–19].

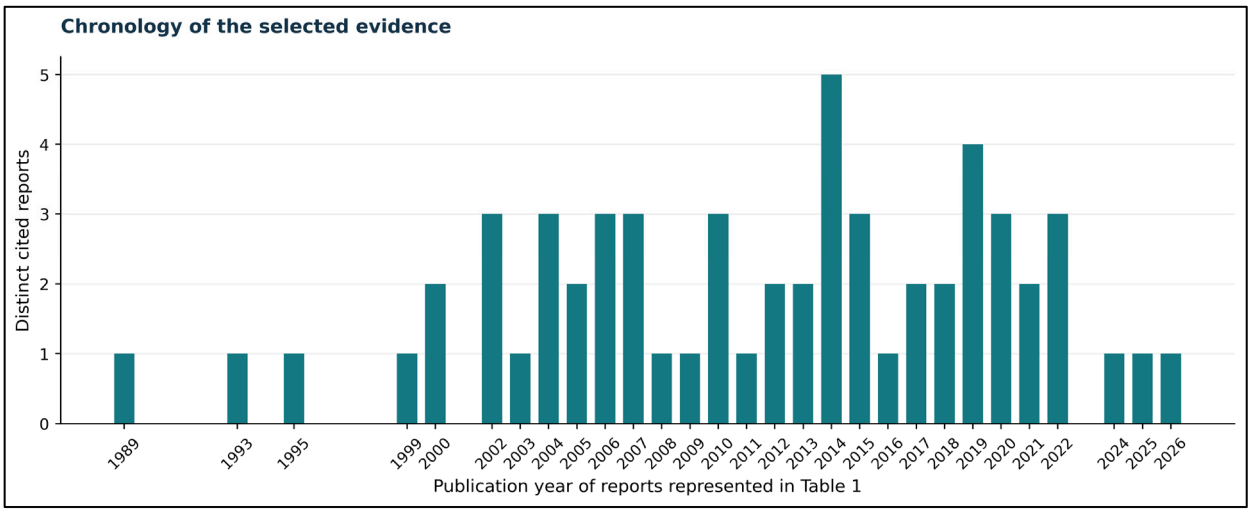


Figure 1. Publication years of distinct cited reports represented in Table 1. Each report is counted once, including reports that contribute several entries. This descriptive chronology is not a systematic publication trend or an account of original compound discovery dates.

Table 1. Marine natural products with anti-ovarian cancer activity.

Compound	Reported Source or Assay Material	Structural Class	Ovarian Cancer Model	Reported Activity and Endpoint	Mechanistic Evidence or Phenotype
Terrein (**1**) [20]	*Aspergillus terreus* PF26	Polyketides	SKOV-3 primary human ovarian cancer cells ovarian cancer stem-like cells	ND; cell viability decreased to 68% at 10 mg/L and 53% at 15 mg/L	G2/M arrest
Kaneoheoic acid I (**2**) [21]	*Fusarium graminearum* FM1010	Polyketides	A2780	IC_{50} = 18.52 μM	A2780 antiproliferation and NF-κB reporter inhibition measured separately
Verticillin A (**3**) [16]	Fungal strain MSX59553; marine provenance of ovarian-study material not established	Peptides	OVSAHO OVCAR-4 OVCAR-8 Ovarian xenograft model	IC_{50} = 60 nM IC_{50} = 47 nM IC_{50} = 45 nM	Oxidative stress, DNA damage and altered histone modifications; G9a involvement proposed
7β-hydroxycholesterol-1β-carboxylic acid (**4**) [22]	*Aspergillus* sp. BM05	Steroids	A2780 A2780 CisR	IC_{50} = 10.0–100.0 μM	No specific downstream target reported
7β-hydroxycholesterol (**5**) [22]					
7α-hydroxycholesterol (**6**) [22]					
Ergosterol-5α,8α-peroxide (**7**) [22]					
Viomellein (**8**) [23]	*Aspergillus ochraceus*	Quinones	A2780	IC_{50} = 5.0μM	ND
Ochratoxin B (**9**) [23]		Alkaloids		IC_{50} = 3.0μM	
Bromophilone B (**10**) [24]	*Penicillium canescens*	Polyketides	A2780	IC_{50} = 2.7μM	ND
Citromycin (**11**) [25]	*Sporothrix* sp.	Polyphenols	SKOV-3 A2780	No cytotoxicity under tested conditions; migration/invasion inhibition at 5–25 μM	ERK1/2 pathway inhibition, downregulates MMP-2/MMP-9, anti-metastasis
Versixanthone N (**12**) [26]	*Aspergillus versicolor* HDN1009	Polyketides	HO-8910	IC_{50}: 1.7–16.1 μM	ND
Versixanthone O (**13**) [26]					
Biscognienyne M (**14**) [27]	*Aspergillus* sp GXNU QG1a	Polyphenols	A2780	IC_{50} = 6.8μM	ND
Versixanthone G (**15**) [28]	*Aspergillus versicolor* HDN1009	Polyketides	HO-8910	IC_{50} = 9.6 μM	Cell cycle blockade, Topo I inhibition
Versixanthone H (**16**) [28]				IC_{50} = 6.9 μM	Topo I inhibition
Versixanthone L (**17**) [28]				IC_{50} = 1.5 μM	ND
Versixanthone M (**18**) [28]				IC_{50} = 1.4 μM	ND
Chaetoglobosin K (**19**) [29]	*Diplodia macrospora; marine* provenance not established in cited study	Macrolides	A2780/CP70 OVCAR-3 Angiogenesis assays	Reduced cell viability from 0.5 μM (A2780/CP70) and 1 μM (OVCAR-3); angiogenesis inhibition	Reduced viability and angiogenesis; Akt/HIF-1α/VEGF-associated effects

Table 1. *Cont.*

Compound	Reported Source or Assay Material	Structural Class	Ovarian Cancer Model	Reported Activity and Endpoint	Mechanistic Evidence or Phenotype
3-HT (**20**) [30]	Aspergillus-associated metabolite; marine provenance of cited ovarian-study material not established	Polyphenols	A2780 CP70 OVCAR-3	ND, 16 µM, inhibition 66%	ROS/MAPK signal regulation, S-phase arrest
Brocazine G (**21**) [31]	*Penicillium brocae* MA-231	Peptides	A2780 A2780 CisR	IC_{50} = 664 nM IC_{50} = 661 nM	Retained cytotoxicity in A2780 CisR; cisplatin resensitization not established
Photopiperazine A (**22**) [32]	AJS-327	Peptides	SKOV3	Light-sensitive isomer mixture; IC_{50} not assigned to individual isomer	ND
Photopiperazine B (**23**) [32]				Light-sensitive isomer mixture; IC_{50} not assigned to individual isomer	
Photopiperazine C (**24**) [32]				Light-sensitive isomer mixture; IC_{50} not assigned to individual isomer	
Photopiperazine D (**25**) [32]				Light-sensitive isomer mixture; IC_{50} not assigned to individual isomer	
Lagumycin B (**26**) [33]	*Micromonospora* sp.	Quinones	OVCAR-4, Kuramochi	ND	ND
Dehydrorabelomycin (**27**) [33]				ND	
Phenanthroviridone (**28**) [33]				ND	
WS-5995 A (**29**) [33]				LC_{50} = 18.6 µM against Kuramochi	
N-(2-hydroxyphenyl)-2-phenazinamine (**30**) [34]	Marine actinomycete BM-17	Quinones	COC1	IC_{50} = 28.11 µg/mL	ND
Cysrabelomycin (**31**) [35]	*Streptomyces* sp. HN-A124	Alkaloids	A2780	IC_{50} = 10.23 µM	ND
Marmycin A (**32**) [36]	*Streptomyces*-related actinomycete CNH990	Quinones	A2780	ND, 5 µM, inhibition 68%	G1 phase arrest
Marmycin B (**33**) [36]					ND
Urukthapelstatin A (**34**) [37]	*Mechercharimyces asporophorigenens* YM11-542	Peptides	OVCAR-3, OVCAR-4, OVCAR-5, OVCAR-8, SKOV-3	Potent nanomolar cytotoxicity toward multiple ovarian cancer cell lines in NCI-60 panel	ND
Coibamide A (**35**) [38]	*Leptolyngbya cyanobacteria*	Peptides	OVCAR-3, OVCAR-4, OVCAR-5, OVCAR-8, SKOV-3	GI_{50}: 3.8–110 nM	Sec61α binding and inhibition of ER protein import established in separate mechanistic studies [39]
Hectochlorin (**36**) [40]	*Lyngbya majuscula*	Macrolides	A2780 SKOV-3	IC_{50} = 20 nM	Promotes actin hyperpolymerization leading to antiproliferative activity

Table 1. *Cont.*

Compound	Reported Source or Assay Material	Structural Class	Ovarian Cancer Model	Reported Activity and Endpoint	Mechanistic Evidence or Phenotype
Myrocin D (**37**) [41]	*Arthrinium* sp. from the sponge *Geodia cydonium*	Terpenoids	A2780 A2780 CisR	IC_{50} = 41.3 µM	ND
Myrocin A (**38**) [41]				IC_{50} = 28.2 µM	
Norlichexanthone (**39**) [41]				IC_{50} = 68.2 µM	
Anomalin A (**40**) [41]				IC_{50} = 4.34 µM	Potent activity against cisplatin-resistant cells
Rac-dibromophakellstatin (**41**) [42]	*Phakellia mauritiana*	Alkaloids	OVXF 899L	IC_{50} = 0.6 µM	ND
1-Deoxysecofascaplysin A (**42**) [43]	*Thorectandra* sp.	Alkaloids	OVCAR-3	IC_{50} = 2.2 µg/mL	ND
24-homoscalarolide A (**43**) [44]	*Carteriospongia*	Terpenoids	A2780	IC_{50} = 0.65 µM	Antiproliferative activity; molecular target not established
12-acetoxy-24-homoscalarolide B (**44**) [44]				IC_{50} = 0.26 µM	Antiproliferative activity; direct target not established
12-hydroxy-24-homoscalarolide A (**45**) [44]				IC_{50} = 0.28 µM	Antiproliferative activity; within-series SAR reported
24-homoscalarolide D (**46**) [44]				IC_{50} = 4.5 µM	Antiproliferative activity; within-series SAR reported
seco-24-homoscalarolide A (**47**) [44]				IC_{50} = 8.7 µM	Antiproliferative activity; within-series SAR reported
Dysidaminones A–M (**48**–**60**) [45]	*Dysidea fragilis*	Terpenoids	SK-OV-3	IC_{50}: 2.89–73.4 µM	Selected analogues inhibited NF-κB in a separate reporter assay; ovarian-cell mechanism not established
Aminoquinones 14–18 in the source report (**61**–**65**) [45]				IC_{50}: 4.81–9.38 µM	
Gukulenin A (**66**) [46]	*Phorbas gukhulensis*	Terpenoids	A2780, SKOV-3, OVCAR-3, TOV-21G, A2780 xenograft mice	IC_{50}: 0.03–0.36 µM	Induce apoptotic cell death
Stelliferin riboside (**67**) [47]	*Rhabdastrella globostellata*	Terpenoids	A2780	IC_{50} = 7.3 µM	ND
3-epi-29-acetoxystelliferin E (**68**) [47]				IC_{50} = 27 µM	
Stellettin J (**69**) [47]				IC_{50} = 1.2 µM	
Stellettin K (**70**) [47]				IC_{50} = 0.28 µM	
Lehualide B (**71**) [48]	*Plakortis*	Polyketides	IGROV-ET	GI_{50} = 0.83 µM	Antiproliferative activity; target not established in cited isolation study
Lehualide D (**72**) [48]				GI_{50} = 0.73 µM	Antiproliferative activity; target not established
Leiodolide A (**73**) [49]	*Leiodermatium*	Macrolides	OVCAR-3	GI_{50} = 0.25 µM	Cytotoxicity reported; microtubule mechanism not established in cited isolation study
Zampanolide (**74**) [50]	*Cacospongia mycofijiensis*	Macrolides	1A9	IC_{50} = 14.3 ± 2.4 nM	stabilizes microtubules and blocks cells in G2/M
Mycalamide A (**75**) [51]	*Mycale Theonella*	Polyketides	Murine M5076 ovarian sarcoma	ND, resulted in an ILS of 118%	Protein synthesis inhibition

Table 1. *Cont.*

Compound	Reported Source or Assay Material	Structural Class	Ovarian Cancer Model	Reported Activity and Endpoint	Mechanistic Evidence or Phenotype
Scleritodermin A (**76**) [52]	*Scleritoderma nodosum*	Peptides	A2780	IC_{50} = 0.94 μM	Inhibited tubulin polymerization
Microcionamide A (**77**) [53]	*Clathria basilana*	Peptides	A2780	IC_{50}:0.45—28 μM	ND
Microcionamide C (**78**) [53]					
Microcionamide D (**79**) [53]					
Phakellistatin 2 conformer A (**80**) [54]	*Stylotella aurantium*	Peptides	A2780	IC_{50} = 2.72 nM	ND
Phakellistatin 2 conformer B (**81**) [54]				IC_{50} = 1.12 nM	
Aragusterol A (**82**) [55]	*Xestospongia* sp.	Steroids	SKOV-3	IC_{50} = 0.43 μM	ND
Laulimalide (**83**) [56]	*Cacospongia mycofijiensis*	Macrolides	SKOV-3	IC_{50} = 11.53 ± 0.53 nM	Microtubule stabilization
Peloruside A (**84**) [57]	*Mycale hentscheli*	Macrolides	A2780 A2780AD	IC_{50} = 66 ± 21 nM IC_{50} = 455 ± 79 nM	Microtubule stabilization
Discodermolide (**85**) [58,59]	*Discodermia dissoluta*	Polyketides	SKOV-3, SKOV-3 xenograft mice	IC_{50} = 8.2 ± 3.8 nM; potentiation of paclitaxel in ovarian xenografts	Microtubule stabilization; potentiation of paclitaxel in ovarian xenografts
Smenothiazole A (**86**) [60]	*Smenospongia aurea*	Peptides	A2780	IC_{50} = 10–30 nM	Cell-cycle and apoptotic responses reported; model-specific mechanism requires verification
Smenothiazole B (**87**) [60]				IC_{50} = 50–70 nM	
Peyssonoic acid A (**88**) [61]	*Peyssonnelia*	Terpenoids	A2780/DDP-S	IC_{50} = 34.5 μM	ND
Peyssonoic acid B (**89**) [61]				IC_{50} = 13.5 μM	
19-O-β-D-glucopyranosyl-19-hydroxy-cholest-4-en-3-one (**90**) [62]	*Peyssonnelia*	Steroids	A2780/DDP-S	IC_{50} = 1.39 μM	Antiproliferative activity; direct molecular target not established
19-O-β-D-N-acetyl-2-aminoglucopyranosyl-19-hydroxy-cholest-4-en-3-one (**91**) [62]				IC_{50} = 1.35 μM	Antiproliferative activity; direct molecular target not established
Dieckol (**92**) [63]	*Ecklonia cava*	Polyphenols	A2780 SKOV-3	IC_{50} = 84.3 μg/mL	ROS/AKT pathway regulation, induces apoptosis
Piericidin A1 (**93**) [64]	*Streptomyces* sp. BRA-035	Polyketides	OVCAR-8	Reported IC_{50} = 0.0005 nM (500 fM); exceptionally low value requires independent confirmation	ND
Ionostatin (**94**) [65]	*Streptomyces* sp. AJS-327	Polyketides	SKOV3	IC_{50} = 7.4 μg/mL	ND
Diazaquinomycin A (**95**) [66]	*Streptomyces* sp. F001	Quinones	OVCAR5	LC_{50} = 8.8 μM	DNA-damage-associated responses and p21 upregulation examined for diazaquinomycin A
Diazaquinomycin E (**96**) [66]			OVCAR5	LC_{50} = 9.0 μM	Cytotoxicity; mechanism not established for this analogue

Table 1. *Cont.*

Compound	Reported Source or Assay Material	Structural Class	Ovarian Cancer Model	Reported Activity and Endpoint	Mechanistic Evidence or Phenotype
Dictyostatin (**97**) [67]	*Spongia* sp.	Macrolides	1A9PTX10 1A9PTX22	GI_{50} = 3.2 ± 2.4 nM GI_{50} = 1.3 ± 1.0 nM	Drives the conversion of cellular soluble tubulin pools into microtubules
Isolaulimalide (**98**) [56]	*Cacospongia mycofijiensis*	Macrolides	SK-OV-3 SKVLB-1	IC_{50} = 2.57 ± 0.29 μM; IC_{50} = 2.65 ± 1.384 μM	Antiproliferative and microtubule-related effects
Lamellarin D (**99**) [68]	*Lamellaria* sp.	Alkaloids	IGROV IGROV-ET	Topo I inhibition; cell-line-specific potency depends on assay	Stabilization of Topo I–DNA complex and DNA cleavage
Plitidepsin (**100**) [69]	*Aplidium albicans*	Peptides	TOV-21G	ND	eEF1A2-associated effects in ovarian clear-cell carcinoma models
Squalamine (**101**) [70]	*Squalus acanthias*	Steroids	OV2008 OV2008-HER2 CAOV3	ND	Anti-angiogenic effects; enhanced cisplatin effects in ovarian xenografts
Pectenotoxin II (**102**) [71]	*Poecillastra* sp. *Jaspis* sp.	Macrolides	IGROV1 OVCAR-3	$LC_{50} = 6.73 \times 10^{-8}$ M $LC_{50} = 6.16 \times 10^{-8}$ M	ND
Hymenialdisine (**103**) [17]	*Acanthella*	Alkaloids	A2780S	IC_{50} = 146.8 μM	ND
Polyketides 6–12 in the source report (**104–110**) [72]	*Trichoderma* sp. FM652	Polyketides	A2780	IC_{50} = 0.5–8.07 μM	ND
Bryostatin-1 (**111**) [73]	*Bugula neritina*	Macrolides	Recurrent/persistent epithelial ovarian cancer; combination with cisplatin	Two partial responses among 8 patients; toxicity limited the tested regimen	PKC modulator
Didemnin B (**112**) [74]	*Tridemnum solidum*	Peptides	Previously treated epithelial ovarian cancer	No objective responses among 16 evaluable patients; significant toxicity	Clinical activity assessment; direct target not tested in this trial
Malformin A1 (**113**) [17]	*Aspergillus* spp.; commercial assay material; marine provenance not established	Peptides	A2780S A2780CP	IC_{50} = 0.23 μM IC_{50} = 0.34 μM	ND
Lamellarin O (**114**) [75]	*Ianthella* sp.	Alkaloids	2008/MRP1	ND	Weak Inhibitor of MRP1
Fucoidan (**115**) [76]	*Phaeophyceae*	Others	SKOV-3 Caov-3	ND	G0/G1 arrest
Trabectedin (**116**) [77]	*Ecteinascidia turbinata*	Alkaloids	The phase III OVA-301 trial	Trabectedin + PLD in platinum-sensitive subgroup (PFI > 6 mo): PFS 9.2 vs. 7.5 mo (HR 0.73; 95% CI 0.56–0.95; P = 0.017))	DNA minor-groove alkylation [12]

Note: PLD = pegylated liposomal doxorubicin, PFI = platinum-free interval, PFS = progression-free survival, HR = hazard ratio, CI = confidence interval, mo = months. ND = not determined or not reported for the specified endpoint; CisR = cisplatin-resistant; DDP = cisplatin; DDP-S = cisplatin-sensitive; ILS = increase in lifespan. IC_{50}, GI_{50}, and LC_{50} describe different endpoints and are not directly interchangeable. Values obtained in different models or exposure conditions should not be used to rank compounds. Ranges reported for compound groups are retained as ranges and are not assigned to individual compound–cell pairs. Biological source denotes the reported isolation source or assay-material provenance, not necessarily the biosynthetic producer. Contextual entries with unestablished marine provenance are identified explicitly.

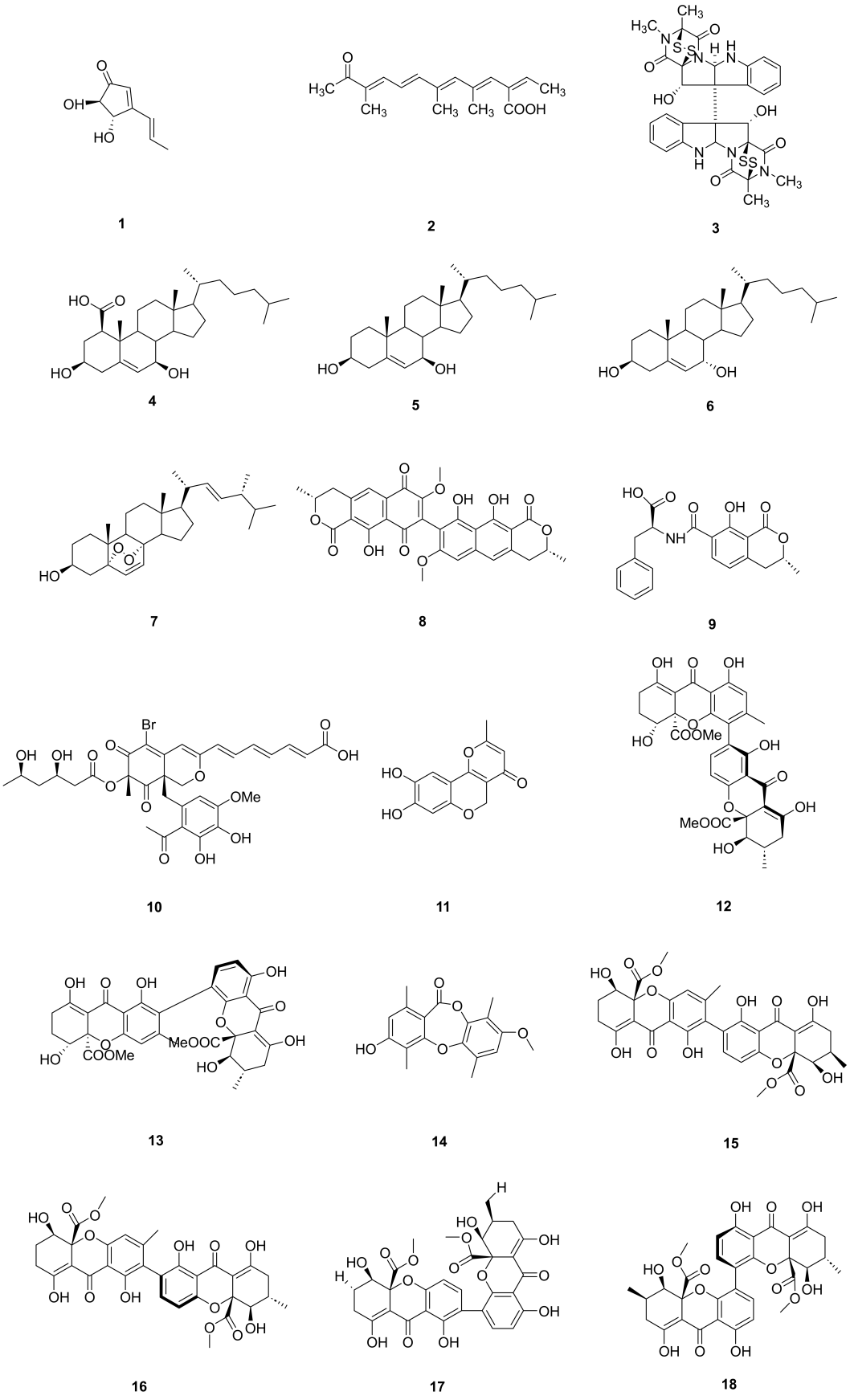


Figure 2. *Cont.*

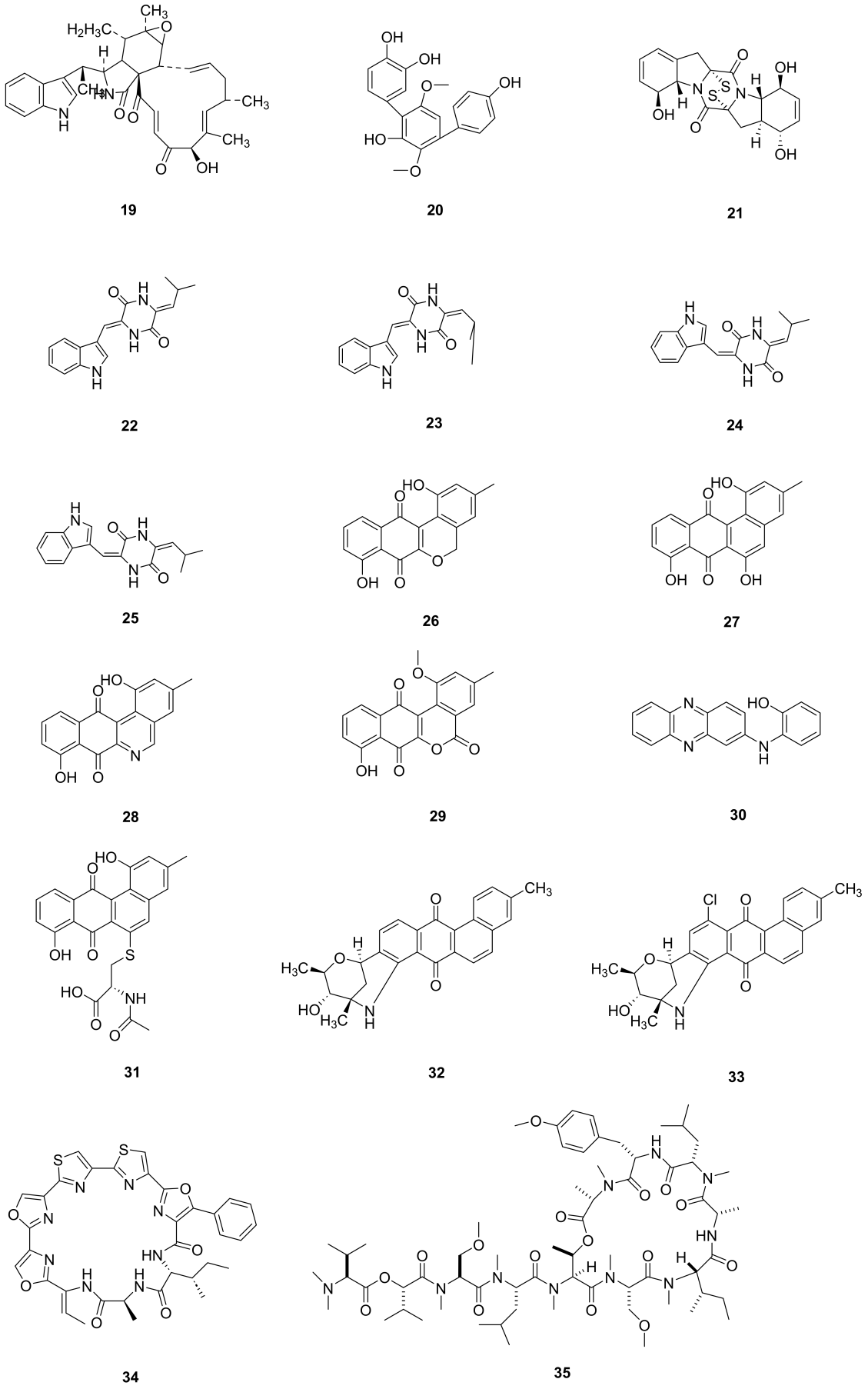
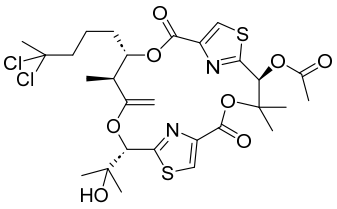
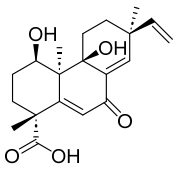


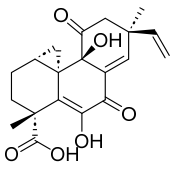
Figure 2. *Cont.*



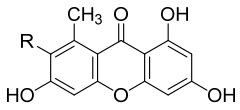
36



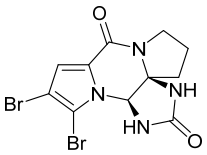
37



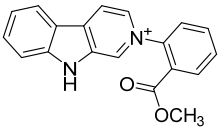
38



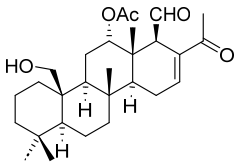
39 R=H
40 R=OH



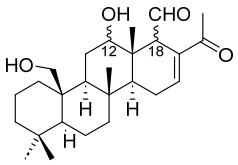
41



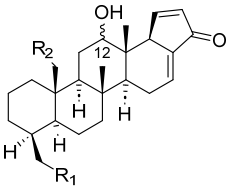
42



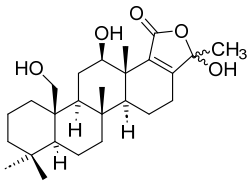
43



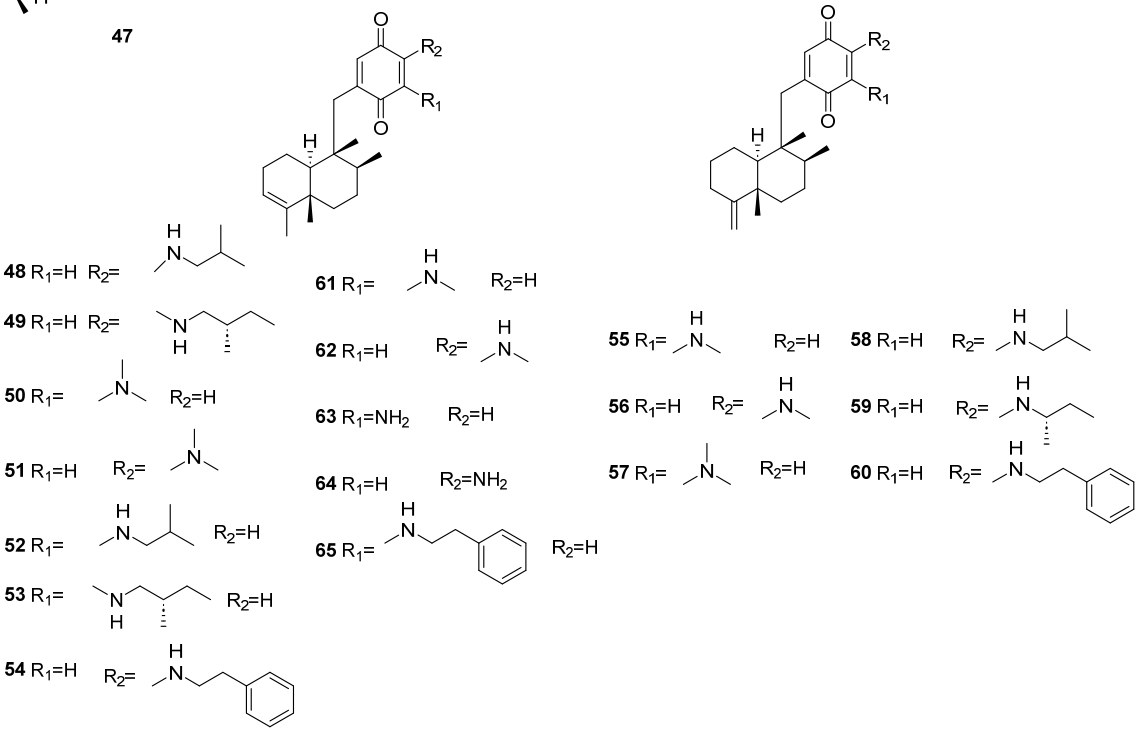
44 12α-OH,18α-CHO
45 12β-OH,18β-CHO



46 R_1=H,R_2=OH,12β-OH



47



48 R_1=H R_2=
49 R_1=H R_2=
50 R_1= R_2=H
51 R_1=H R_2=
52 R_1= R_2=H
53 R_1= R_2=H
54 R_1=H R_2=
61 R_1= R_2=H
62 R_1=H R_2=
63 R_1=NH_2 R_2=H
64 R_1=H R_2=NH_2
65 R_1= R_2=H
55 R_1= R_2=H
56 R_1=H R_2=
57 R_1= R_2=H
58 R_1=H R_2=
59 R_1=H R_2=
60 R_1=H R_2=

Figure 2. *Cont.*

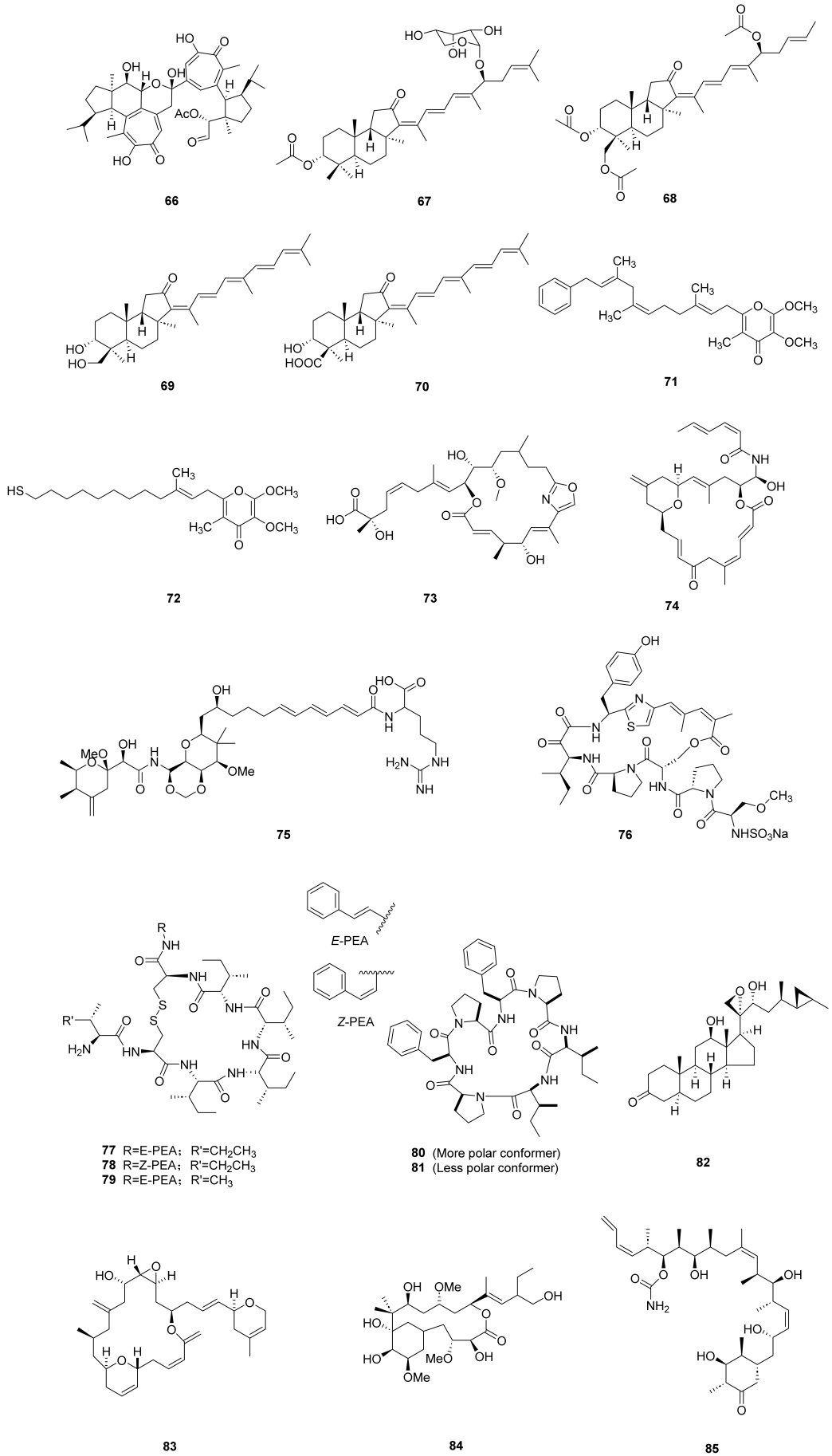


Figure 2. *Cont.*

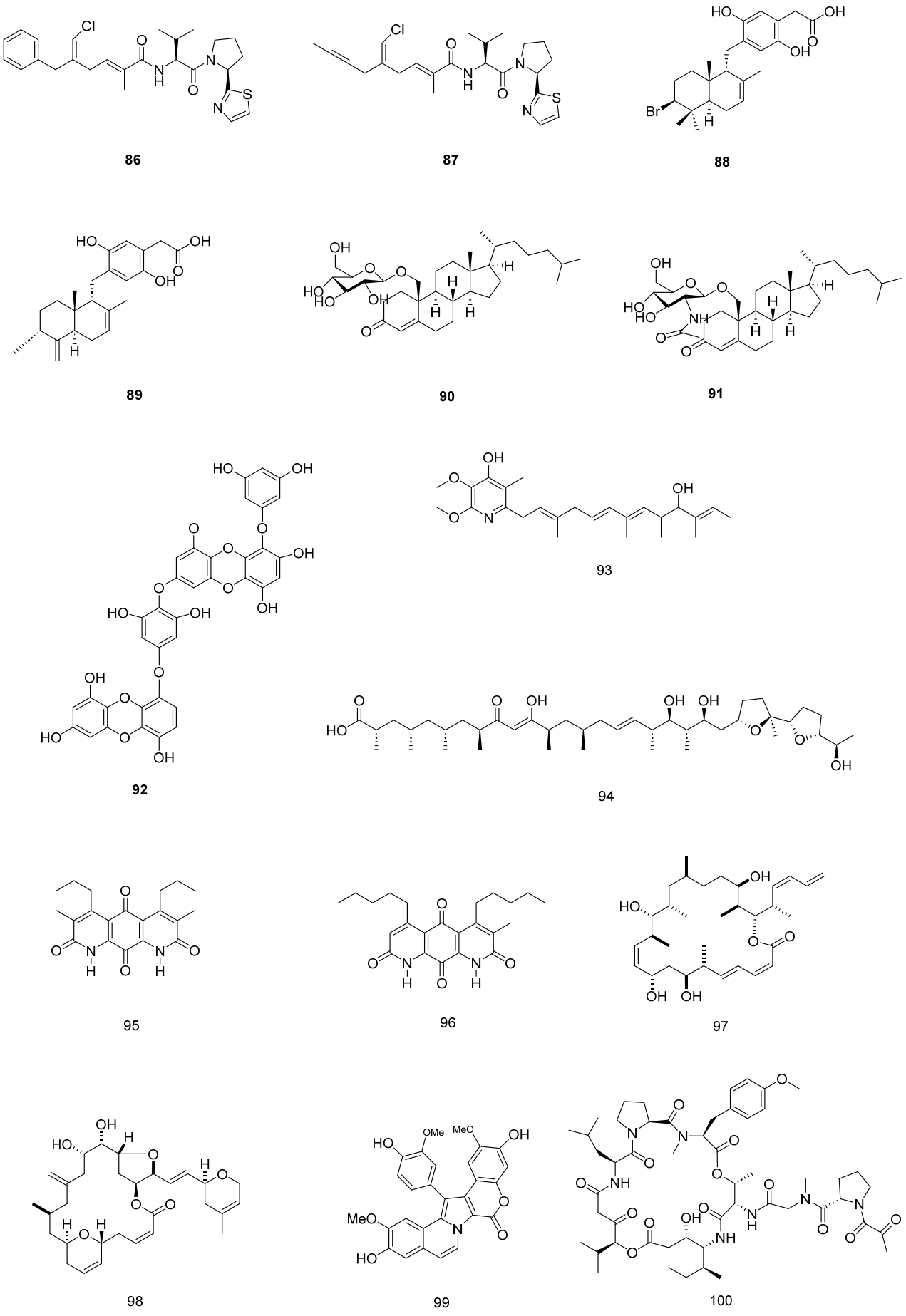


Figure 2. *Cont.*

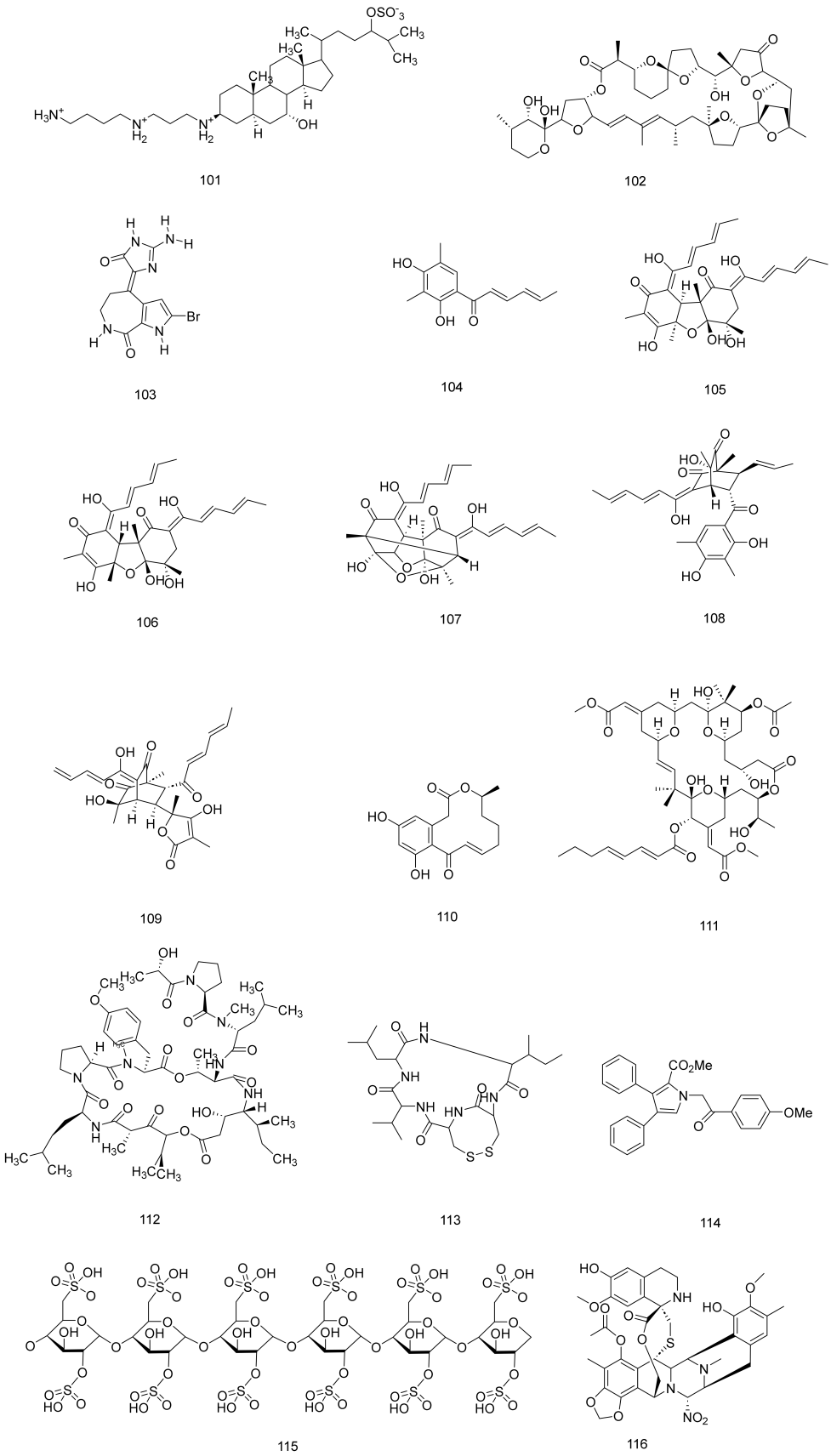


Figure 2. Structures and numbered entries in the selected inventory (**1**–**116**). Compound groups and conformers retain the numbering used in Table 1. Fucoidan (**115**) denotes a polysaccharide preparation rather than a single chemically defined small molecule.

Table 1 covers terpenoids, steroids, peptides, polyketides, quinones/polyphenols, macrolides, and other structural classes. Figure 3 describes the composition of this selected inventory rather than estimating scaffold prevalence across the literature. Within these broad classes, individual compounds have distinct mechanisms, including microtubule stabilization, oxidative-stress modulation, epigenetic changes, and inhibition of invasion. Mechanistic assignments therefore rest on compound-specific experiments, not structural classification alone [16,25,46,50,63].

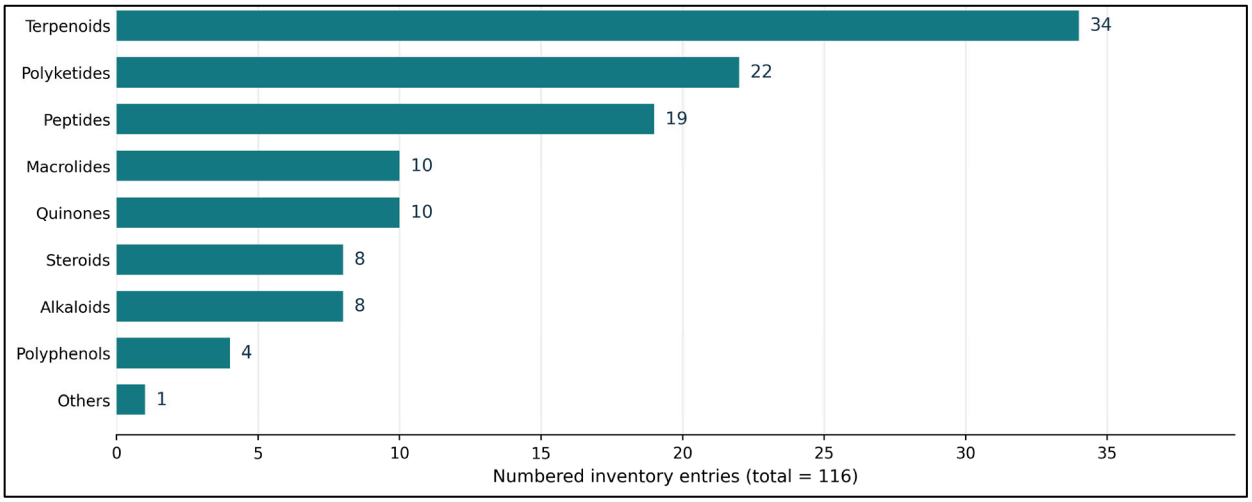


Figure 3. Structural-class assignments for the 116 numbered entries in Table 1. Grouped numbered analogues are expanded, and reported conformers are counted as numbered entries. Categories are working labels rather than mutually exclusive biosynthetic classes; counts do not represent unique scaffolds or independent experiments.

2. Marine Natural Products with Anti-Ovarian Cancer Activity

2.1. Anti-Ovarian Cancer Natural Products Isolated from Marine Fungi

Marine-derived fungi from mangroves, sponges, coral-associated habitats, and sediments produce diverse metabolites for cancer research. The term "marine-derived" refers to the isolation context; it does not establish that a strain is exclusively marine or that its metabolites occur only in marine environments. Ecological conditions and interspecies interactions can shape metabolite production, although linking a particular environmental pressure to an anticancer effect requires direct experimental evidence [18,23,24].

Fungal metabolites studied in ovarian cancer models include polyketides, terpenoids, alkaloids, peptide-derived compounds, and steroids. These categories overlap: xanthones and many quinones are polyketide-derived, while diketopiperazines can be described as both peptide-derived metabolites and alkaloids. We therefore use structural labels to organize the discussion rather than to predict mechanism. Highly oxygenated aromatic cores, fused rings, and sulfur-containing heterocycles provide useful starting points for structure–activity studies, but target specificity must be tested experimentally [23,24,78].

Terrein (**1**), isolated from the sponge-associated fungus *Aspergillus terreus* PF26, inhibited proliferation and induced G2/M arrest in human ovarian cancer models, including stem-like cell populations [20]. These observations support further investigation of its effects on mitotic progression; they do not establish selective eradication of ovarian cancer stem cells. Kaneoheoic acid I (**2**), from *Fusarium graminearum* FM1010, inhibited A2780 proliferation (IC_{50} = 18.52 μM) and TNF-α-induced NF-κB reporter activity in a separate assay (IC_{50} = 15.86 μM) [21]. Linking these findings requires pathway perturbation in the

ovarian model, because parallel activity in two assays does not demonstrate that NF-κB inhibition mediates the antiproliferative response.

Epigenetic regulation and oxidative stress have been investigated in studies of verticillin A (**3**), an epipolythiodioxopiperazine fungal metabolite. In high-grade serous ovarian cancer models, verticillin A showed nanomolar cytotoxicity, induced oxidative stress and DNA damage, altered histone modification profiles, and promoted apoptosis [16]. Inhibition of histone methyltransferases, including G9a, is a proposed contributor, but the ovarian study did not establish G9a as the sole causal target. Encapsulation in expansile nanoparticles reduced tumor burden and liver toxicity relative to the free compound in mice. The ovarian study used fungal strain MSX59553; marine occurrence and the provenance of material used in anticancer assays should therefore be distinguished [16,79].

Citromycin (**11**), isolated from the Antarctic marine-derived fungus *Sporothrix* sp., illustrates an anti-invasive effect that is separable from cytotoxicity. It inhibited migration and invasion of SKOV3 and A2780 cells without measurable cytotoxicity under the tested conditions, reduced EMT-associated marker expression and MMP-2/9 activity, and suppressed ERK1/2 signaling. Ectopic ERK expression counteracted the anti-invasive effect, providing functional evidence for involvement of this pathway [25].

Dimeric tetrahydroxanthones from *Aspergillus versicolor* HDN1009 illustrate the need to distinguish scaffold-level observations from analogue-specific mechanisms. Versixanthones G (**15**) and H (**16**) inhibited HO-8910 cells, with IC_{50} values of 9.6 and 6.9 μM, respectively. The reported Topo I inhibition and cell-cycle effects concern selected tested dimers and should not be assigned to the entire series. Versixanthones L (**17**) and M (**18**) were more potent in the reported cellular assay (IC_{50} = 1.5 and 1.4 μM, respectively), but their direct molecular targets remain unresolved [28]. Greater cellular potency therefore does not necessarily indicate stronger Topo I engagement.

Brocazine G (**21**), a bisthiodiketopiperazine from the mangrove-derived fungus *Penicillium brocae* MA-231, showed similar potency in parental A2780 and cisplatin-resistant A2780 CisR cells (IC_{50} = 664 and 661 nM, respectively) [31]. This result indicates limited cross-resistance in that paired model. It does not demonstrate restoration of cisplatin sensitivity, which would require combination experiments and evidence that the resistant phenotype is modified. The example illustrates why resistance-model activity should be reported separately from resistance reversal.

Chaetoglobosin K (**19**) reduced ovarian-cancer-cell-induced angiogenesis and altered Akt/HIF-1α/VEGF-associated signaling [29]. The cited study also reported reduced ovarian cancer cell viability; describing the compound as noncytotoxic would therefore be inaccurate. Moreover, the marine provenance of the assay material is not established in that study. Chaetoglobosin K is retained here as a contextual fungal comparator, with its provenance limitation stated in Table 1, rather than presented as unequivocal evidence for a marine-derived anti-angiogenic agent.

The fungal literature includes compounds with antiproliferative and anti-invasive activity, as well as candidates whose in vivo performance depends on formulation. Further development will require compound-specific target validation, testing in appropriate ovarian histotypes, assessment of nonmalignant-cell toxicity, and reliable production. Genome-guided discovery and controlled cultivation can expand the accessible metabolite repertoire, but new chemical diversity is most valuable when paired with pharmacological assays that can distinguish meaningful activity [16,23–25].

2.2. Anti-Ovarian Cancer Natural Products Isolated from Marine Actinomycetes and Bacteria

Marine bacteria, including actinomycetes and cyanobacteria, produce peptides, macrolides, quinones, phenazines, and hybrid polyketide–peptide metabolites. Biosyn-

thetic gene clusters provide a basis for investigating this diversity, as illustrated by the specialized-metabolite capacity of *Salinispora tropica* [80]. Several bacterial metabolites are active at nanomolar concentrations in ovarian cancer assays, but differences in assay design prevent a general potency ranking against metabolites from other sources [81].

The cellular targets of bacterial and cyanobacterial metabolites vary widely and cannot be inferred from biological origin. Coibamide A, for example, inhibits Sec61-dependent protein translocation, whereas hectochlorin promotes actin assembly [39,40]. When ovarian cancer sensitivity data and target-identification experiments come from different cellular systems, each dataset needs to be interpreted within its own experimental context.

Photopiperazines A–D (**22**–**25**), isolated from the marine-derived actinomycete strain AJS-327, are photosensitive, interconverting diketopiperazines [32]. Their interconversion complicates both potency assignment and structure–activity interpretation. Activity measured for an isomeric mixture should not be attributed independently to each component, and the selectivity highlighted in the original report concerned glioblastoma models. Ovarian activity should therefore be interpreted from the relevant assay data rather than extrapolated from another tumor type.

Angucycline-related metabolites include phenanthroviridone (**28**) and marmycins A and B (**32**, **33**), which have been evaluated in ovarian cancer assays [33,36]. Marmycin A was associated with modest apoptosis and G1 arrest in the original study [36]. These observations support a cellular response phenotype but do not establish a common target across angucyclines. Likewise, mechanistic findings for marmycin A should not be assigned automatically to marmycin B.

Urukthapelstatin A (**34**), isolated from *Mechercharimyces asporophorigenens* YM11-542, displayed nanomolar growth-inhibitory activity in the NCI-60 panel, including ovarian cancer cell lines [37]. Its heterocycle-rich macrocycle offers a scaffold for medicinal chemistry and target-identification studies. However, cellular potency alone does not establish a particular binding partner, ovarian selectivity, or a favorable therapeutic window.

Cyanobacterial metabolites extend the available mechanisms beyond conventional DNA-directed cytotoxicity. Coibamide A (**35**), originally isolated from *Leptolyngbya* sp., showed differential antiproliferative activity across the NCI-60 panel [38]. Subsequent chemical-proteomic and biochemical studies identified Sec61α as a direct binding target and demonstrated inhibition of secretory and membrane protein biogenesis [39]. Those experiments were not restricted to ovarian cancer models, so ovarian-specific dependency remains a separate question. Hectochlorin (**36**), isolated from *Lyngbya majuscula*, promotes actin assembly [40], illustrating that cytoskeletal effects should not be equated exclusively with tubulin inhibition.

Chemical accessibility is as important as pharmacological activity in the development of bacterial metabolites. Complex structures and low yields can limit mechanistic experiments and dose-intensive animal studies. Heterologous expression may improve access to selected compounds, but production depends on pathway architecture, host compatibility, and process optimization. The presence of a biosynthetic gene cluster alone does not establish scalability or product stability, both of which warrant early evaluation [82].

Additional candidates include piericidin A1 (**93**) from *Streptomyces* sp. BRA-035, ionostatin (**94**) from strain AJS-327, and diazaquinomycins A and E (**95**, **96**) from strain F001 [64–66]. Their reported activities use different endpoints and units. The exceptionally low OVCAR-8 IC_{50} reported for piericidin A1 (500 fM) is retained as a source-reported result, but should motivate independent dose–response confirmation and scrutiny of dilution, assay interference, and exposure conditions before prioritization [64]. It should not serve as the basis for a cross-study potency ranking.

Bacterial metabolites are especially useful as leads when defined chemical activity can be linked to a validated molecular interaction, as in the case of coibamide A and Sec61 [39]. Such a link provides a concrete basis for biomarker studies and analogue design. Genome mining can further expand the candidate pool, although its therapeutic value will ultimately depend on reproducible activity, selectivity, and exposure in relevant ovarian cancer models [80,82].

2.3. Anti-Ovarian Cancer Natural Products from Marine Sponges

Marine sponges are a well-established source of bioactive polyketides, terpenoids, alkaloids, and peptides [83]. Their associated microorganisms can contribute substantially to the observed chemistry. Studies of *Entotheonella* demonstrate that metabolites isolated from a sponge may originate from bacterial symbionts [19]. Here, "sponge-associated" refers to the isolation source unless a biosynthetic producer has been established. This distinction affects both ecological interpretation and the choice of a sustainable production strategy.

The sponge-associated compounds in Table 1 encompass several structural classes and affect proliferation, apoptosis, cytoskeletal organization, and drug response. These observations justify further study of individual compounds but do not show that sponge metabolites are inherently more complex, potent, or mechanistically diverse than fungal or bacterial metabolites. The most convincing examples combine cellular activity with biochemical or structural evidence.

Terpenoids isolated from *Carteriospongia* spp. and *Rhabdastrella globostellata* inhibited ovarian cancer cell proliferation, with some reported IC_{50} values below 1 μM [44,47]. Sesquiterpene aminoquinones from *Dysidea fragilis* were also active against SK-OV-3 cells [45]. These series offer opportunities for matched structure–activity analysis. However, activity differences should be interpreted within the same assay, and NF-κB reporter effects should not be treated as direct target identification or assumed to explain ovarian-cell cytotoxicity. Several sponge-associated natural products stabilize microtubules, including zampanolide (**74**), laulimalide (**83**), peloruside A (**84**), and discodermolide (**85**) [50,56–58]. Their binding modes differ: laulimalide and peloruside A occupy an external non-taxane site on β-tubulin, whereas zampanolide covalently modifies residues within the luminal taxane site [84,85]. Discodermolide and dictyostatin also interact with the taxoid-binding region [59,67]. Retained activity in selected resistant cell lines therefore cannot be explained by a shared non-taxane binding site.

Peptide-derived sponge metabolites include scleritodermin A (**76**), microcionamides A, C, and D (**77**–**79**), and two reported conformers of phakellistatin 2 (**80**, **81**) [52–54]. Their ovarian-cell activity supports further investigation of cyclic peptide scaffolds, but conformers should be distinguished from independently defined chemical entities. Scleritodermin A was reported to inhibit tubulin polymerization [52], whereas the direct targets of other entries remain incompletely characterized. Cyclic architecture alone does not establish target affinity or tumor selectivity.

Gukulenin A (**66**), a sponge-derived tetraterpenoid, has been examined in both ovarian cancer cells and xenograft mice [46]. Submicromolar cellular activity and tumor-growth inhibition provide evidence beyond an initial screen. The absence of substantial bodyweight loss under the tested conditions is reassuring but does not define a therapeutic window or exclude organ toxicity. These findings warrant exposure-linked efficacy and tolerability studies rather than a claim of clinical superiority over cisplatin.

Aragusterol A (**82**) provides another example of a defined cellular phenotype: its activity was associated with G1 arrest [55]. Such effects complement microtubule-directed mechanisms but should be distinguished from direct binding to cyclins or CDKs. Similarly, activity reported for aminoquinones and other sponge metabolites should remain

linked to the compound and assay tested, rather than generalized into a shared multitarget mechanism [45,47,55].

For sponge-associated leads, mechanistic differentiation needs to be considered alongside supply and exposure. Non-taxane-site microtubule stabilizers offer one source of pharmacological differentiation, while other scaffolds may reveal distinct cellular vulnerabilities. Progress will also depend on sustainable production, feasible synthesis, and testing in histotype-appropriate ovarian cancer models [11,19,82].

The distinction among tubulin-binding modes is especially relevant to resistance studies. Laulimalide and peloruside A occupy an external non-taxane site, whereas zampanolide reacts covalently within the taxane site [84,85]. These differences generate hypotheses about cross-resistance; they do not guarantee activity against every taxane-resistant or platinum-resistant tumor. Resistance mechanisms must be defined in the model used.

2.4. Anti-Ovarian Cancer Natural Products from Marine Algae

Marine algae yield polyphenols, terpenoids, sterol glycosides, and polysaccharides that require different analytical and pharmacological approaches. A defined small molecule can be characterized by molar concentration and purity, whereas a polysaccharide preparation also requires information on molecular-weight distribution and composition. Neither marine origin nor occurrence in an edible alga guarantees safety at an anticancer exposure [63,76,86].

Peyssonoic acids A and B (**88**, **89**), sesquiterpene hydroquinones isolated from the red alga *Peyssonnelia* sp., were investigated for both ecological activity and inhibition of ovarian cancer cell proliferation [61]. Their reported A2780/DDP-S IC_{50} values were 34.5 and 13.5 μM, respectively. These findings identify bioactive scaffolds but provide limited information about a therapeutic target, selectivity, or activity in resistant disease.

Two sterol glycosides (**90**, **91**) isolated from *Peyssonnelia* sp. inhibited proliferation of A2780/DDP-S cells, with reported IC_{50} values of 1.39 and 1.35 μM, respectively [62]. Structure–activity experiments implicated the C-3 α,β-unsaturated ketone and C-19 oxygenation in activity; the molecular target and any role in membrane signaling remain to be established.

Dieckol (**92**), a phlorotannin from *Ecklonia cava*, has more extensive mechanistic support than many other algal entries. In SKOV3 cells, dieckol increased ROS, disrupted mitochondrial function, activated caspases, and inhibited AKT and p38 signaling. Antioxidant treatment and overexpression experiments partially counteracted these responses, supporting pathway involvement rather than identifying AKT or p38 as direct binding targets. Reduced SKOV3 xenograft growth adds in vivo evidence, although pharmacokinetic and comprehensive safety data remain necessary for development [63].

Algal metabolites include chemically distinct small molecules and polysaccharides, and their activities cannot be summarized by a single toxicity profile. Fucoidan (**115**), a sulfated polysaccharide preparation, inhibited proliferation and induced G0/G1 arrest and apoptosis in SKOV-3 and Caov-3 cells, with changes in PI3K/Akt-associated signaling [76]. Such results support further preclinical investigation but do not establish efficacy or safety in patients.

For both dieckol and fucoidan, preparation identity and exposure need to be linked to reproducible biological effects. Combination experiments should include appropriate single-agent controls, defined treatment schedules, and assessment in nonmalignant cells. These controls are particularly important when benefit is attributed to broad pathway modulation rather than to a validated direct target [63,76].

Recent work extends the algal evidence beyond tumor-cell apoptosis. Dieckol, 7-phloroeckol, and 8,8′-bieckol from *Ecklonia cava* were investigated in ovarian cancer cells and tumor-associated macrophage models. The reported responses involved IL-17RA/Act1-

associated signaling and context-dependent ERK1/2 activation, with altered MMP and TIMP-1 expression. Docking and molecular dynamics proposed IL-17RA binding, but this remains a computational interaction hypothesis rather than experimentally demonstrated direct engagement. The ERK response also cautions against assigning a single direction of pathway regulation to a compound across different biological settings [87].

Figure 4 shows the biological-source distribution of the selected inventory. The counts depend on the compounds and classification rules used here and do not measure discovery productivity or clinical value. Table 1 also includes candidates from tunicates, a bryozoan, and a shark, together with fungal assay materials for which marine provenance was not established in the cited ovarian studies. Microbial production by sponge symbionts adds a further complication to assigning biological origin [19,69,70,73,74].

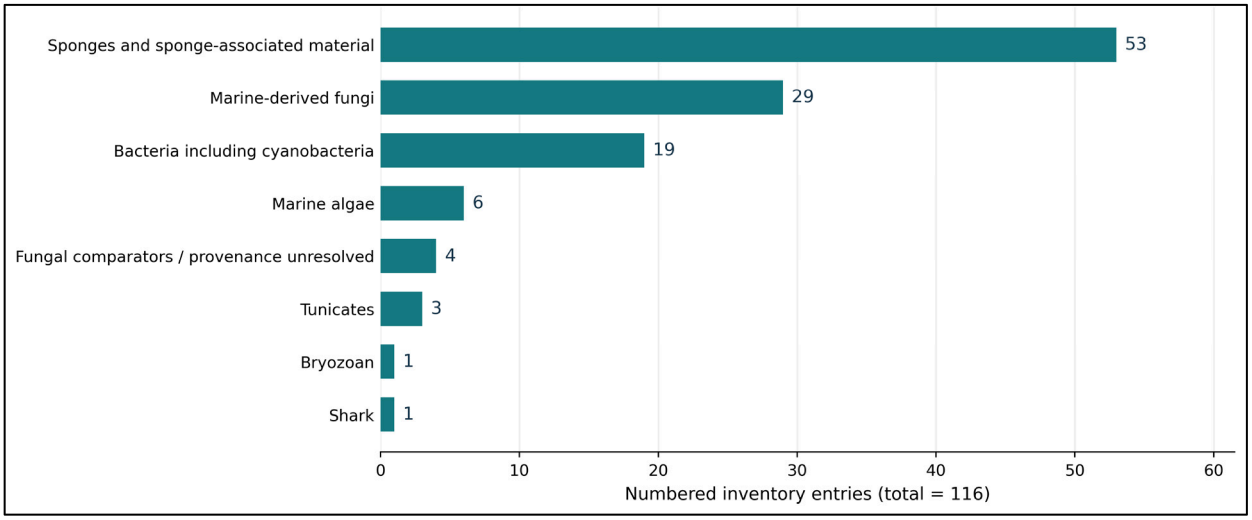


Figure 4. Source assignments for the 116 numbered entries in Table 1. Each numbered entry is counted once by isolation source or assay-material provenance. Four fungal entries (**3**, **19**, **20**, **113**) are separated because marine provenance of the cited ovarian-study material is not established. Isolation host is distinguished from biosynthetic producer; counts do not measure source productivity or clinical value.

2.5. Comparative Analysis of Marine-Derived Natural Products Against Ovarian Cancer

The major source groups provide complementary scaffolds, but biological origin alone cannot rank their pharmacological value. Table 2 compares their reported characteristics and practical constraints. Candidate selection requires a balanced assessment of mechanism, model relevance, selectivity, supply, and exposure rather than reliance on the lowest IC_{50} drawn from unrelated experiments [11,88].

Fungal metabolites offer tractable examples of proliferation arrest, altered oxidative stress, and inhibition of invasion. Terrein (**1**), verticillin A (**3**), and citromycin (**11**) illustrate different response phenotypes, not a uniform fungal mechanism [16,20,25]. Fermentation may support supply, but production yield, genetic stability, and the provenance of assay material need to be established for each candidate.

Marine bacterial metabolites include highly active peptide-derived and polyketide scaffolds. Urukthapelstatin A (**34**) illustrates potent cellular activity, while coibamide A (**35**) provides a more developed link to a direct target [37,39]. The photopiperazines (**22**–**25**) illustrate a different issue: light-dependent interconversion can limit interpretation of activity and complicate chemical standardization [32]. These distinctions are more informative for development than a general claim that bacterial metabolites are more cytotoxic than fungal metabolites.

Table 2. Comparative characteristics of marine natural products with anti-ovarian cancer activity.

Marine Source	Major Structural Classes	Representative Compounds	Reported Biological Effects	Development Opportunities	Current Limitations
Marine fungi	Polyketides, xanthones, diketopiperazines, meroterpenoids	Terrein (**1**), citromycin (**11**), brocazine G (**21**); verticillin A (**3**) as a provenance-qualified comparator	Cell-cycle effects, apoptosis, invasion inhibition; compound-specific evidence	Chemical diversity; preclinical apoptosis and invasion studies	Variable production yields; target and exposure gaps
Marine bacteria & actinomycetes	Peptides, angucyclines, phenazines, diketopiperazines	Urukthapelstatin A (**34**), marmycin A (**32**), photopiperazines (**22**–**25**), coibamide A (**35**)	Compound-specific cytotoxicity, cell-cycle effects; Sec61 inhibition for coibamide A	Potent cellular activity for selected compounds; validated target for coibamide A	Complex biosynthesis and synthesis
Marine sponges	Macrolides, terpenoids, steroids, cyclic peptides	Zampanolide (**74**), Peloruside A (**84**), Gukulenin A (**66**)	Microtubule stabilization or inhibition, apoptosis; compound-specific evidence	Diverse scaffolds; activity in selected resistant models	Limited natural supply
Marine algae	Polyphenols, sterol glycosides, terpenoids	Dieckol (**92**), Peyssonoic acids A (**88**) Peyssonoic acids B (**89**)	ROS-mediated apoptosis, AKT/p38 modulation	Distinct small molecules and polysaccharides; safety requires testing	Limited exposure data; preparation heterogeneity for polysaccharides

Sponge-associated metabolites are notable for the range of experimentally investigated cytoskeletal interactions. Laulimalide (**83**) and peloruside A (**84**) bind an external non-taxane site, while zampanolide (**74**) covalently modifies the luminal taxane site [84,85]. Their development value lies in these mechanistic distinctions and the resistance profiles they generate. Low natural abundance and complex synthesis remain important constraints.

Algal entries include defined small molecules and heterogeneous polysaccharide preparations. Dieckol (**92**) provides cellular rescue experiments and xenograft data, whereas the interpretation of fucoidan (**115**) depends additionally on preparation characteristics [63,76]. Neither example supports a source-wide claim of low toxicity or suitability for long-term treatment.

Cross-study comparisons are constrained by differences in tumor model, endpoint, exposure time, and compound preparation. Even apparently similar IC_{50} values may not be directly comparable. Prioritization is more defensible when based on reproducible pharmacology, target engagement, resistance profiles, supply, pharmacokinetics, and toxicity than on taxonomy or a single potency measurement [11,88].

Shared phenotypes such as apoptosis, cell-cycle arrest, altered invasion, or reduced angiogenesis do not imply a shared direct target. They can arise from different primary interactions or from secondary stress responses. Network analysis and multi-omics are useful for generating mechanistic hypotheses, but causal attribution still requires orthogonal target-engagement measurements and perturbation of the proposed dependency [11,39].

A useful comparison identifies the principal uncertainty for each lead. A potent compound with an unknown target may require target deconvolution; a mechanistically defined scaffold may lack validation in ovarian models; and a candidate with animal efficacy may need exposure or safety optimization. Addressing these specific gaps provides a clearer development rationale than ranking compounds by taxonomic origin.

2.6. Other Marine Sources and Contextual Comparators

The inventory also includes tunicate-derived plitidepsin (**100**) and didemnin B (**112**), bryostatin-1 (**111**) from a bryozoan, and the shark-derived aminosterol squalamine (**101**) [69,70,73,74]. These entries extend the source coverage beyond the four principal

groups, but their evidence ranges from preclinical studies to small clinical trials and does not support a common development classification. The tunicate-derived trabectedin (**116**) [77] is included in Table 1 and discussed alongside lurbinectedin in Section 5.2. The inventory is not intended as an exhaustive catalogue of clinical agents.

Several fungal entries also require a provenance qualification. Verticillin A was tested using strain MSX59553 in the cited ovarian study, and the ovarian reports for chaetoglobosin K and commercially sourced malformin A1 do not establish marine provenance for the assay material [16,17,29]. These entries are retained for mechanistic context and explicitly qualified, rather than counted as unambiguous evidence of a marine source–ovarian activity connection.

3. Molecular Mechanisms of Marine Natural Products Against Ovarian Cancer

Marine-derived natural products affect several cellular processes involved in ovarian cancer progression and treatment resistance, including apoptosis, cell-cycle progression, invasion, angiogenesis, and drug-response pathways. The supporting evidence ranges from phenotypic assays to mechanistic perturbation and animal studies. Changes in multiple signaling markers, on their own, do not demonstrate simultaneous engagement of multiple direct targets [16,25,29,39].

We group the evidence into five response categories: apoptosis, cell-cycle regulation, invasion-associated plasticity, angiogenesis, and activity in resistant models. Table 3 summarizes these categories separately from direct target classes, while Figure 5 maps representative compounds to the available types of mechanistic evidence rather than depicting a comprehensive signaling network. Section 3.7 and Table 4 address recent work on ferroptosis-associated responses and macrophage signaling; these studies are not included in the fixed numbered inventory in Table 1.

Table 3. Molecular mechanisms of marine natural products against ovarian cancer.

Mechanism	Representative Compounds	Targets, Pathways, or Markers	Biological Outcomes
Apoptosis	Verticillin A (**3**), Dieckol (**92**), Gukulenin A (**66**)	ROS, mitochondrial and caspase-associated responses; direct targets not established	Programmed cell death
Cell-cycle arrest	Terrein (**1**), marmycin A (**32**), aragusterol A (**82**), versixanthones G/H (**15**, **16**), 3-HT (**20**)	Compound-specific cell-cycle and Topo I-associated effects; marker changes do not establish direct CDK inhibition	G1, S or G2/M arrest, depending on compound and model
Invasion-associated effects	Citromycin (**11**) [25]	ERK1/2 and EMT-associated markers; reduced MMP-2/9 activity	Reduced migration and invasion in vitro
Anti-angiogenesis	Chaetoglobosin K (**19**); provenance-qualified comparator, squalamine (**101**) [29,70]	Akt/HIF-1α/VEGF-associated signaling for chaetoglobosin K; angiogenesis assays for squalamine	Reduced angiogenesis
Activity in resistant models	Peloruside A (**84**), Zampanolide (**74**), Brocazine G (**21**) [31,57,84]	Compound-specific tubulin interactions; Brocazine G target unresolved	Retained activity; resensitization not established by cytotoxicity alone
Epigenetic regulation	Verticillin A (**3**)	Altered histone marks; G9a involvement proposed [16]	Oxidative stress, DNA damage, apoptosis; formulation-dependent xenograft efficacy

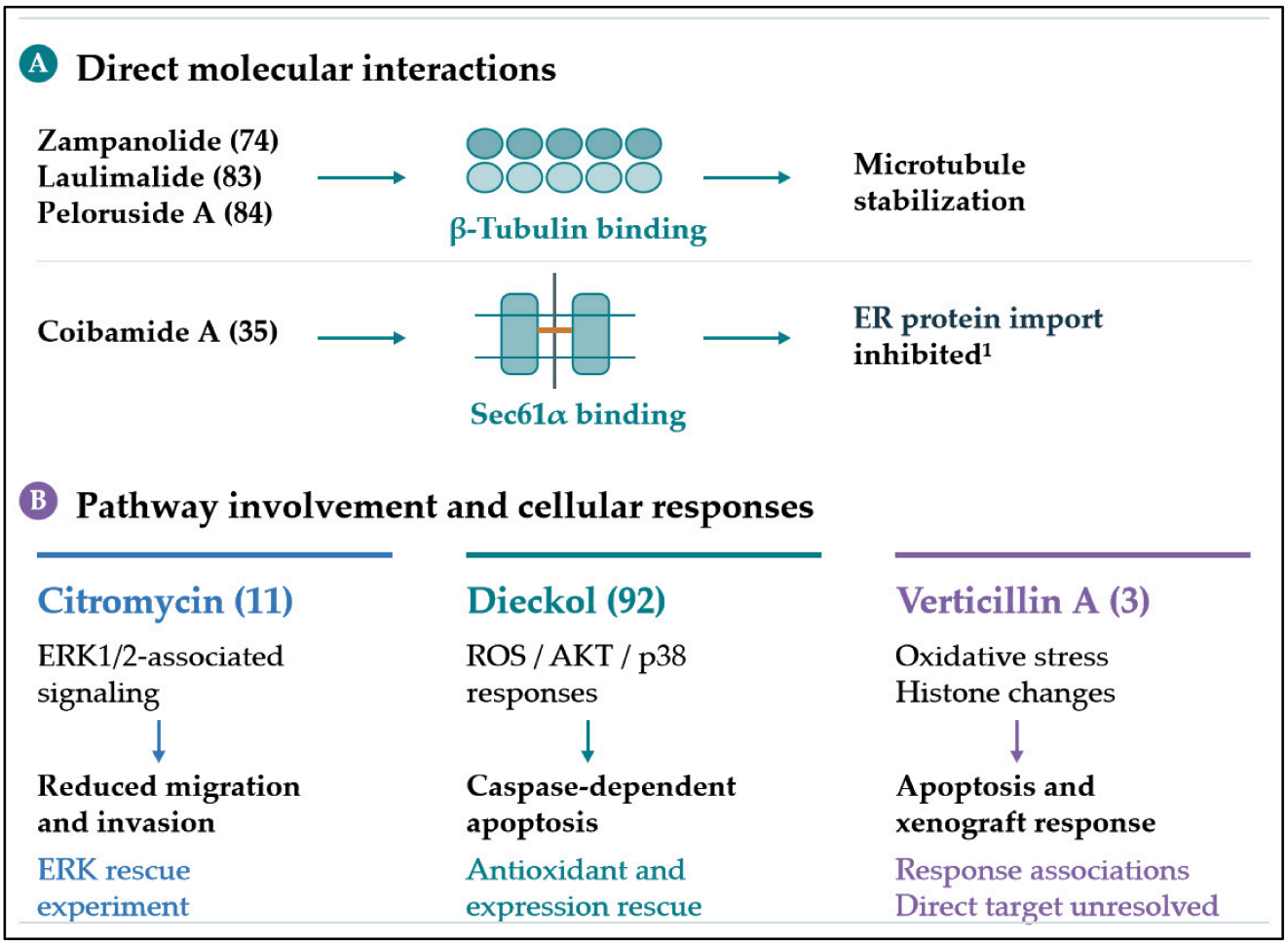


Figure 5. Mechanisms and the evidence supporting them. Direct molecular interactions are separated from pathway involvement. (**A**) Direct molecular interactions: Zampanolide, laulimalide, and peloruside A bind β-tubulin to stabilize microtubules; coibamide A binds Sec61α to inhibit ER protein import. (**B**) Pathway involvement and cellular responses. Citromycin suppresses migration and invasion via ERK1/2 signaling, confirmed by an ERK rescue assay. Dieckol induces caspase-dependent apoptosis through ROS/AKT/p38 pathways. Verticillin A triggers oxidative stress and histone alterations, resulting in apoptosis and xenograft response, while its direct target remains unknown.[1] Sec61 target studies extend beyond ovarian models. Symbols are schematic. Sources: [20,24,61,81,85,86].

3.1. Induction of Apoptosis

Several natural products induce apoptosis in ovarian cancer models. Dieckol (**92**) increased ROS, disrupted mitochondrial function, and activated caspases; antioxidant treatment and overexpression of AKT or p38 partially counteracted these effects [63]. Verticillin A (**3**) induced oxidative stress, DNA damage, and apoptosis in high-grade serous ovarian cancer cells, together with changes in histone modifications [16]. Gukulenin A (**66**) elicited apoptotic responses and inhibited xenograft growth, whereas marmycin A (**32**) was associated with modest apoptosis and G1 arrest [36,46]. These findings support apoptosis as an important response, but they do not point to a single ROS/mitochondrial pathway shared by all marine metabolites.

3.2. Regulation of Cell-Cycle Progression

Cell-cycle effects vary among marine natural products. Terrein (**1**) induced G2/M arrest, whereas marmycin A (**32**) and aragusterol A (**82**) were associated with G1 ar-

rest [20,36,55]. Such redistribution does not, by itself, demonstrate direct inhibition of a cyclin or CDK. Target-level evidence is stronger for selected microtubule stabilizers: laulimalide (**83**) and peloruside A (**84**) bind an external non-taxane site, while zampanolide (**74**) binds covalently within the taxane site [84,85]. Distinguishing cell-cycle phenotypes from demonstrated tubulin interactions is essential for mechanistic interpretation and for evaluating resistance.

3.3. Inhibition of EMT and Tumor Metastasis

EMT-associated plasticity can contribute to migration, invasion, and treatment response, but marker changes alone do not demonstrate suppression of metastasis [89]. Citromycin (**11**) reduced migration and invasion in SKOV3 and A2780 cells at tested non-cytotoxic concentrations, accompanied by reduced EMT-associated markers, MMP-2/9 activity, and ERK1/2 signaling [25]. These observations support an anti-invasive phenotype in vitro. Evidence from peritoneal dissemination models would be needed to establish an antimetastatic effect in vivo.

Ectopic ERK expression counteracted the anti-invasive effect of citromycin, providing functional evidence that this pathway contributes to the response [25]. The rescue experiment is more informative than a change in ERK phosphorylation alone, although it does not identify ERK as the compound's direct binding target. Comparable rescue or genetic perturbation studies are needed before the mechanism can be extended to other metabolites.

3.4. Suppression of Angiogenesis

The clinical benefit of bevacizumab in GOG-0218 establishes angiogenesis as a relevant therapeutic target in ovarian cancer [90], but it does not validate any particular marine compound. In preclinical experiments, chaetoglobosin K (**19**) reduced ovarian-cell-induced angiogenesis through an Akt/HIF-1α/VEGF-associated pathway [29]. Squalamine (**101**) also inhibited angiogenesis and enhanced cisplatin effects in ovarian xenograft models, providing a separate example of a marine-derived anti-angiogenic candidate [70].

3.5. Activity in Resistant Models and Chemotherapy Resensitization

Resistance studies need to answer three separate questions: does the candidate retain activity in a resistant model, does it restore sensitivity to the original drug, and does the proposed resistance mechanism explain the combination response? Similar brocazine G potency in paired A2780 models addresses only the first question [31]. The wentilactone A study examined cisplatin response together with NF-κB/ECM1-associated signaling and therefore provides a more direct assessment of resensitization [91]. Reporting these outcomes separately avoids conflating activity with resistance reversal.

Combination experiments are more informative when they use concentration matrices and defined treatment schedules rather than a single combination dose. The interaction model should be specified in advance, and the effect of the combination must be compared with that of each agent alone. Genetic or pharmacological perturbation of the proposed resistance pathway can then test causality. Figure 6 brings together this interpretation framework and the compound-specific tubulin-binding differences relevant to cross-resistance [31,84,85,91].

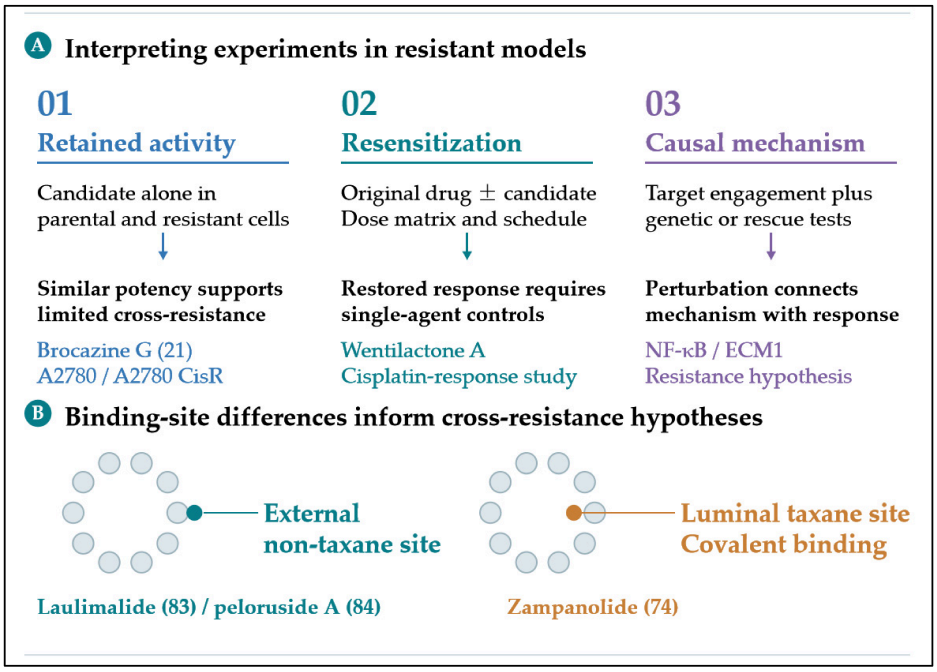


Figure 6. Experimental interpretation of resistance studies and schematic microtubule-binding sites. (**A**) Retained activity, drug resensitization, and causal attribution require different evidence. Brocazine G IC_{50} values in parental and resistant A2780 models are source-reported values from [31], not new measurements; similar potency does not establish restoration of cisplatin sensitivity. (**B**) External non-taxane-site binding by laulimalide/peloruside A and covalent luminal taxane-site binding by zampanolide. Cross sections are schematic and not to scale; binding-site differences do not guarantee escape from a particular resistance mechanism. Sources: [31,57,84,85,91].

3.6. Distinguishing Direct Targets from Downstream Responses

Different experiments support different levels of mechanistic inference. Changes in ROS, phosphorylation, or apoptosis markers demonstrate association; rescue experiments support functional pathway involvement; and binding, structural, or chemical-proteomic measurements can establish direct interactions. Coibamide A–Sec61 studies and structural analyses of tubulin-binding agents provide target-level evidence, whereas citromycin–ERK rescue experiments establish pathway involvement without identifying a direct binding partner [25,39,84,85]. These forms of evidence complement one another but are not interchangeable.

A proposed mechanism also needs to explain the phenotype in an appropriate ovarian cancer model. Target engagement observed in another tumor type can guide experiments but does not establish histotype-specific dependence. Orthogonal assays, relevant genetic perturbation, and exposure-matched controls would add more mechanistic value than simply expanding panels of downstream markers [11,88,92].

3.7. Recent Evidence on Regulated Cell Death and the Tumor Microenvironment

Gukulenin A has recently been examined with olaparib in ovarian cancer cells. Increased oxidative stress and lipid peroxidation accompanied the combination response; antioxidant treatment, NADPH oxidase inhibition or perturbation, and ferrostatin-1 rescue supported an oxidative-stress-dependent ferroptosis component. ERK overexpression partially attenuated the effect. These cellular perturbation experiments strengthen the mechanistic interpretation of the combination but do not identify a direct gukulenin A target or demonstrate clinical reversal of PARP-inhibitor resistance [93].

Fucoxanthin from *Laminaria japonica* was evaluated in A2780 and SKOV3 cells and a xenograft model. The study associated AMPK/Nrf2/HMOX1 signaling with ferroptosis

and reported markers of apoptosis, pyroptosis, and necroptosis under the PANoptosis framework. Proteomic prioritization and docking were complemented by cellular thermal shift and drug-affinity-responsive target-stability assays, supporting AMPK engagement. Orthogonal biochemical binding and selectivity studies would further define the interaction. Changes in several death-pathway markers should not, by themselves, establish an integrated PANoptotic mechanism [94].

Together with the phlorotannin–macrophage findings [87], these studies extend the mechanistic discussion beyond direct tumor-cell killing. Table 4 summarizes their models and limitations. They update the evidence reviewed here without altering the descriptive denominator used in Figure 1, Figure 3, and Figure 4.

Table 4. Recent primary studies extending the mechanistic scope beyond the numbered inventory.

Candidate and Source	Model and Evidence	Interpretation Limit	Ref.
Gukulenin A; marine sponge	Ovarian cells; olaparib combination; oxidative-stress and ferroptosis rescue experiments	Functional cellular evidence; direct target and clinical efficacy unresolved	[93]
Fucoxanthin; *Laminaria japonica*	Ovarian cells and xenograft; AMPK CETSA/DARTS; regulated-death-associated markers	Engagement evidence does not establish binding selectivity or integrated PANoptosis	[94]
Dieckol and related phlorotannins; *Ecklonia cava*	Ovarian cells and macrophage models; IL-17RA/Act1 and ERK-associated responses	Predicted IL-17RA binding requires experimental validation	[87]

4. Therapeutic Potential and Clinical Translation of Marine Natural Products Against Ovarian Cancer

4.1. Levels of Evidence and the Transition from Preclinical Data to Clinical Claims

The therapeutic claims attached to marine natural products need to match the evidence available. In vitro cytotoxicity, activity in drug-resistant cells, xenograft efficacy, and benefit in randomized clinical trials represent different levels of support. Plitidepsin (**100**), for example, showed eEF1A2-associated antitumor effects in ovarian clear-cell carcinoma models, including chemoresistant cells and xenografts [69]. These results support further preclinical investigation in this histotype rather than a general clinical claim.

Activity in a resistant model is a useful screening result, but it is not synonymous with reversal of chemotherapy resistance. Brocazine G (**21**) showed similar potency in parental A2780 and A2780 CisR cells, while the distinct tubulin interactions of peloruside A (**84**) and zampanolide (**74**) can limit cross-resistance in selected models [31,57,84]. Resensitization must be tested in combination with the original drug and with appropriate mechanistic controls, as illustrated by the combined analysis of NF-κB/ECM1 signaling and cisplatin response for wentilactone A [91].

Verticillin A (**3**) shows how formulation can determine whether a potent compound can be evaluated effectively in vivo. Solubility and toxicity complicated its development in high-grade serous ovarian cancer models, whereas expansile nanoparticle delivery improved the preclinical balance between tumor control and liver toxicity [16]. Studies of verticillin analogues and formulations likewise identified stability and tolerability as central issues [79]. This example supports formulation development but does not imply that nanoencapsulation will benefit every candidate or ensure a clinically acceptable safety margin.

Medicinal chemistry is most informative when structural changes are linked to a defined functional assay. Amino-acid-substituted lamellarin D derivatives, for example, showed structure-dependent effects on Topo I-mediated DNA cleavage [68,95]. Such exper-

iments provide a practical basis for optimization beyond structural novelty. For complex marine scaffolds, analogue design needs to integrate target engagement, physicochemical properties, exposure, and synthetic accessibility.

Combination strategies require evidence for each compound and regimen. Discodermolide (**85**) potentiated paclitaxel in ovarian carcinoma xenografts, and squalamine (**101**) was evaluated with cisplatin in ovarian tumor models [58,70]. The recent gukulenin A–olaparib study provides a cellular example of a defined PARP-inhibitor combination [93]. Extending these findings to other metabolites or to immune checkpoint blockade will require interaction, exposure, and toxicity studies. In a small phase II trial, bryostatin-1 (**111**) plus cisplatin produced responses in some patients, but substantial toxicity prevented further evaluation at the tested schedule [73] (Table 5).

Table 5. Therapeutic potential of representative marine natural products against ovarian cancer.

Therapeutic Potential	Representative Compounds	Major Advantages	Current Challenges	Future Development
Activity in resistant models	Brocazine G (**21**), Peloruside A (**84**) [31,57]	Active in resistant models	Limited in vivo evidence	Combination therapy
Targeting microtubules	Zampanolide (**74**), Peloruside A (**84**), Laulimalide (**83**)	Non-taxane-site binding for peloruside A/laulimalide; covalent taxane-site binding for zampanolide [84,85]	Low natural yield, complex total synthesis	Structural optimization
Epigenetic-associated responses	Verticillin A (**3**)	Nanomolar cytotoxicity, altered histone marks and reduced tumor burden with appropriate formulation [16,79]	Potential hepatotoxicity of free Verticillin A, poor water solubility	Target deconvolution, formulation and analogue optimization
Anti-invasive activity	Citromycin (**11**) [25]	Reduced migration/invasion through ERK-associated signaling	Direct target and in vivo dissemination studies needed	Combination with chemotherapy
Anti-angiogenesis	Chaetoglobosin K (**19**); provenance-qualified comparator, squalamine (**101**) [29,70]	Preclinical angiogenesis effects	Limited pharmacokinetics	Exposure-linked efficacy and tolerability studies
Apoptosis induction	Dieckol (**92**), Gukulenin A (**66**)	Apoptotic responses in ovarian models; ROS involvement established for dieckol	Bioavailability	Formulation optimization
Combination adjuvant therapy	Discodermolide (**85**), Squalamine (**101**) [58,70]	Preclinical combinations with paclitaxel or cisplatin; broad PARP-inhibitor synergy not established	Optimal exposure, schedule and tolerability unresolved	Formal interaction analysis and exposure-matched validation

Clinical experience offers an important corrective to expectations based on cellular potency. Didemnin B (**112**) produced no objective responses among 16 evaluable patients with previously treated ovarian cancer and caused clinically important toxicity [74]. Bryostatin-1 combination studies also encountered tolerability constraints [73]. An adequate therapeutic window and a feasible dosing schedule are therefore as important as activity in an ovarian cancer cell line. Most compounds in the present inventory remain at the preclinical stage.

Genome mining and heterologous expression can ease selected discovery and supply constraints, while structure-guided design can support the optimization of chemically accessible analogues [82,96]. Computational screening is most useful when it generates a falsifiable experimental hypothesis. Docking scores and predicted networks do not independently demonstrate binding, ovarian selectivity, or efficacy and cannot substitute for experimental target validation.

The central translational task is to identify candidates whose mechanistic advantages persist at exposures that are both achievable and tolerable. This requires coordinated progress in compound supply, ovarian disease biology, pharmacology, and formulation. Advancement decisions should rest on a defined evidence package rather than on the assumption that chemical novelty will produce clinical benefit [11].

4.2. Marine-Derived Agents in Clinical Development and Their Potential Applications

Clinical trials have evaluated several marine-derived or marine-inspired agents in recurrent ovarian cancer. Trabectedin (ET-743), a tetrahydroisoquinoline alkaloid from the tunicate Ecteinascidia turbinata, is approved in the European Union in combination with pegylated liposomal doxorubicin for platinum-sensitive recurrent ovarian cancer [12,77]. The OVA-301 trial enrolled patients with recurrent disease after first-line platinum-based chemotherapy. The combination improved progression-free survival relative to pegylated liposomal doxorubicin (PLD) alone in the overall population. The difference was statistically significant in the platinum-sensitive subgroup and did not reach statistical significance in the platinum-resistant subgroup [77]. Lurbinectedin (PM01183), a synthetic analogue that shares the DNA-binding mechanism, was studied with atezolizumab in the phase III IMforte trial as maintenance treatment for extensive-stage small-cell lung cancer following first-line induction therapy. The combination improved progression-free and overall survival compared with atezolizumab alone [97]. In ovarian cancer, the phase III CORAIL trial found no progression-free survival advantage over PLD or topotecan in platinum-resistant disease [98]. These trials support reporting the treatment regimen and platinum-sensitivity criteria for each study. Biomarker-directed use of lurbinectedin in ovarian cancer remains investigational.

Other marine-derived compounds have been tested in ovarian cancer patients without reaching approval. Didemnin B produced no objective responses among 16 evaluable patients with previously treated epithelial ovarian cancer and caused clinically important toxicity [74]. Bryostatin-1 combined with cisplatin yielded two partial responses among eight patients, but toxicity limited the regimen that could be delivered [73]. Plitidepsin, the dehydrodidemnin B analogue from *Aplidium albicans*, was approved in Australia with dexamethasone for selected patients with relapsed and refractory multiple myeloma [12,99]. In ovarian cancer, the evidence is preclinical, with eEF1A2-associated activity in clear-cell carcinoma models that included chemoresistant cells and xenografts [69]. Squalamine, an aminosterol from Squalus acanthias, was evaluated with cisplatin in ovarian cancer models [70]. A published phase I study evaluated its safety and pharmacokinetics in patients with advanced cancers [100]. Table 6 summarizes the development stages documented in the cited publications, the ovarian settings in which they have been or could be tested, and the constraints that have limited progress.

Table 6. Clinical development of marine-derived and marine-inspired agents relevant to ovarian cancer.

Compounds	Development Stage in Cited Literature	Ovarian Cancer Evidence	Potential Application in Ovarian Cancer	Principal Limitations
Trabectedin (**116**) [77]	EU approval with PLD for relapsed platinum-sensitive ovarian cancer [12,77]	OVA-301: improved progression-free survival versus liposomal doxorubicin alone; no significant benefit in the platinum-resistant subgroup	Combination partner for platinum-sensitive recurrent disease	Hepatotoxicity, myelosuppression, intravenous administration, complex supply
Lurbinectedin [98]	Phase III IMforte: maintenance with atezolizumab in extensive-stage small-cell lung cancer [97]	CORAIL: no progression-free-survival advantage over liposomal doxorubicin or topotecan in platinum-resistant disease	Investigational biomarker-directed studies and combination strategies	Myelosuppression; no qualified predictive biomarker
Plitidepsin (**100**) [69]	Australian approval with dexamethasone for selected patients with relapsed and refractory multiple myeloma [12,99]	Preclinical activity in clear-cell carcinoma models, including chemoresistant cells and xenografts	Clear-cell histotype-directed studies	Hepatic and muscular toxicity [99]; eEF1A2 dependence not qualified as a biomarker
Didemnin B (**112**) [74]	Phase II clinical trial in patients with previously treated epithelial ovarian cancer	No objective responses among 16 evaluable patients; substantial toxicity	Historical benchmark for depsipeptide development	Narrow therapeutic window; supply and formulation
Bryostatin-1 (**111**) [73]	Phase II with cisplatin; further use at this dose and schedule was limited by toxicity	Two partial responses among eight patients with cisplatin; toxicity limited delivery	Protein kinase C-modulating combination partner	Supply, toxicity, schedule dependence
Squalamine (**101**) [70]	Phase I safety and pharmacokinetic study in advanced cancers [100]	Preclinical anti-angiogenic and cisplatin-enhancing effects in ovarian cancer models [70]	Anti-angiogenic combination	Ovarian clinical efficacy remains unestablished

Three applications follow from this clinical record. The first is trabectedin plus PLD for relapsed platinum-sensitive ovarian cancer, an approved regimen in the European Union [12,77]. The second is to evaluate targeted or local delivery of selected marine-derived cytotoxins. Antibody–drug conjugation and intraperitoneal chemotherapy have clinical precedents in ovarian cancer [101,102]. These studies provide a rationale for evaluating candidate-specific delivery strategies. The third is histotype-directed testing, illustrated by the clear-cell models used to evaluate plitidepsin, in which high-grade serous paradigms may not apply [69,88].

Outside ovarian cancer, marine-derived drugs are already in routine use, including cytarabine, trabectedin, and eribulin mesylate [12,13]. Their existence shows that the limiting factor is not the tractability of marine chemistry but the completeness of the evidence package required for registration. The relevant question for the present inventory is therefore which candidates can be developed to that standard, not whether marine natural products can reach the clinic.

5. Discussion

5.1. Current Challenges and Bottlenecks

The main bottleneck lies between discovering a bioactive metabolite and establishing a credible ovarian cancer lead. The literature contains many activity measurements but far fewer studies that integrate chemical identity, causal mechanism, clinically relevant models, pharmacokinetics, and safety. Candidates merit further investment when these elements are considered together rather than in isolation.

Discovery is also constrained by cultivation. Standard culture conditions recover only part of marine microbial diversity and activate only some biosynthetic pathways, with the recoverable fraction varying by habitat and method. A single universal estimate of this fraction would therefore be misleading. Metagenomic surveys reveal extensive uncharacterized biosynthetic potential, including pathways from uncultivated lineages [103].

Insufficient metabolite supply can delay structure confirmation, mechanistic studies, and adequately powered animal experiments. Uncontrolled batch composition further compromises reproducibility. Fermentation optimization and heterologous production can address some of these constraints, but both require pathway-specific development and analytical verification of product identity and purity [82]. Importantly, supply and chemistry, manufacturing, and controls (CMC) exert stronger constraints on clinical development than on early-stage discovery work. Toxicology studies and early-phase clinical trials require reproducible supplies of characterized material. The amount depends on the compound, formulation, and study design. Scalable production remains a practical constraint for many marine natural products [82]. For complex mixtures such as fucoidan, key quality attributes including molecular-weight distribution, sulfation pattern, and batch-to-batch consistency should be characterized to support reproducible comparisons across batches. The fucoidan study cited here used preclinical ovarian cancer models [76]. Without a robust, qualified supply chain, lot-to-lot physicochemical variability cannot be separated from genuine biological variability.

Model selection remains another limitation. Commonly used ovarian cancer cell lines differ in their genomic similarity to high-grade serous tumors, and no single line represents all ovarian histotypes [88]. Patient-derived organoids can retain clinically relevant heterogeneity and differences in platinum response [92]. Used alongside authenticated cell lines and appropriate nonmalignant comparators, they can improve assessments of selective activity and resistance mechanisms.

Chemical complexity and inadequate in vivo exposure can limit clinical translation. Concentrations that induce apoptosis in cultured cells are often unattainable in plasma or peritoneal fluid under tolerable dosing regimens. The OVA-301 trial illustrates the need to evaluate tolerability alongside efficacy. Neutropenia and transient transaminase elevations were more frequent with trabectedin plus PLD than with PLD alone [77]. Accordingly, preclinical studies should measure dose–exposure relationships, protein binding, and tumor distribution where relevant. Solubility, stability, metabolism, and tissue distribution can prevent a potent in vitro concentration from being reached in tumor tissue. Complex synthesis may also limit the material available for pharmacokinetic and toxicity studies. Supply and exposure therefore need to inform lead selection from the outset, together with mechanism and cellular activity [12,82].

Toxicity defines the usable therapeutic window and represents a major translational barrier. Marine cytotoxins frequently engage targets expressed in normal proliferating tissues. Myelosuppression and hepatic toxicity have been reported with trabectedin-based treatment. Hepatic and muscular toxicity were reported with plitidepsin, and significant toxicities limited the tested ovarian cancer regimens of didemnin B and bryostatin-1 [73,74,77,99]. Preclinical formulation strategies, such as expansile nanoparticle delivery of verticillin A, have reduced liver toxicity in

an ovarian cancer mouse model [16]. Analyses of solid-tumor models also show that nanoparticle delivery to tumors can be limited [104]. Improved tolerability must therefore be validated alongside retained antitumor efficacy and exposure measurements.

Tumor heterogeneity limits broad mechanistic claims because pathway-associated responses may depend on histotype, genotype, or treatment history. Matched resistant models, biomarker-defined cell panels, and patient-derived systems can help distinguish general cytotoxicity from a reproducible vulnerability in a clinically relevant subgroup [88,92]. This heterogeneity also shapes clinical trial design and patient selection, which together determine whether a true therapeutic effect can be detected. CORAIL did not demonstrate a progression-free survival advantage in platinum-resistant ovarian cancer [98]. OVA-301 enrolled patients with recurrent disease and stratified them by platinum sensitivity. The EU indication is for trabectedin with PLD in relapsed platinum-sensitive disease [12,77]. Future trials of marine-derived agents in ovarian cancer should prespecify histotype and include molecular eligibility or stratification criteria, such as BRCA mutation or homologous recombination deficiency status, where supported by the treatment hypothesis. Controlled study designs and pharmacokinetic data can inform endpoint selection, dose, and schedule.

Mechanistic evidence can inform dose selection, biomarker development, and combination design. When the direct target remains unresolved, pharmacokinetic and pharmacodynamic data and functional studies in relevant models can still support prespecified hypotheses. These clinical translational constraints are distinct from the discovery-stage bottlenecks discussed elsewhere, and both categories of challenges form the integrated evidence package summarised in Figure 7 [88,92].

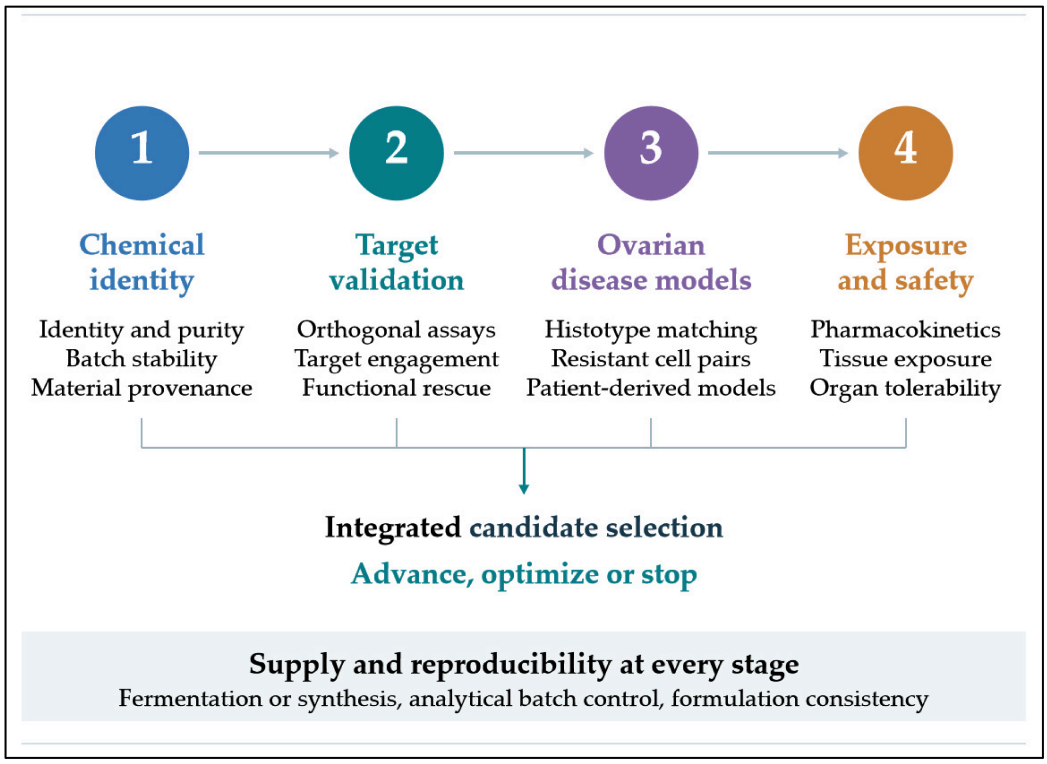


Figure 7. A development framework for marine-derived ovarian cancer leads. Chemical identity, causal mechanism, disease-model relevance, exposure, and tolerability inform integrated candidate selection: advance, optimize, or stop. Supply and reproducibility are required at every stage, and workstreams can proceed in parallel. This diagram describes proposed research decisions rather than completed development milestones. All scientific symbols are schematic. Sources: [11,82,88,92–95].

5.2. Future Perspectives

Future studies will benefit most when technology is applied to a defined development question. Genome-guided discovery can broaden chemical access, synthetic biology can support supply, formulation can alter exposure, and computational tools can prioritize hypotheses. Their value lies in resolving a specific limitation of a candidate, not in novelty alone.

(1) Genome-guided metabolite discovery

Metagenomic analyses of ocean microorganisms have uncovered numerous uncharacterized biosynthetic gene clusters, and antiSMASH provides tools for identifying and annotating candidate pathways [96,103]. These predictions require experimental confirmation through metabolite detection, gene perturbation, or heterologous expression. A predicted cluster does not, by itself, establish production of an anticancer compound [82].

(2) Sustainable production through synthetic biology

Synthetic biology can support metabolite supply through heterologous hosts, pathway refactoring, and metabolic engineering. Success depends on verification of the producing pathway, host compatibility, and reproducible purification. A scalable route to chemically defined active material is a concrete development milestone; low-cost manufacture cannot be assumed before the process has been evaluated [82].

(3) Exposure-guided formulation and delivery

Peritoneal dissemination makes local delivery an attractive research strategy in ovarian cancer. In a preclinical model, verticillin A encapsulated in expansile nanoparticles reduced tumor burden and liver toxicity [16]. Delivery advantages nevertheless depend on the formulation and model. Quantitative studies show that nanoparticle accumulation in tumors is often low, making matched pharmacokinetic and toxicity comparisons essential before assuming improved efficacy or safety [104].

(4) Mechanistically justified combination therapy

Combination therapy is a testable strategy, not a general property of marine natural products. In the randomized OVA-301 trial, trabectedin plus pegylated liposomal doxorubicin improved progression-free survival compared with liposomal doxorubicin alone in recurrent ovarian cancer, but the platinum-resistant subgroup did not show a statistically significant benefit [77]. By contrast, the phase III CORAIL trial found no progression-free survival advantage for lurbinectedin over pegylated liposomal doxorubicin or topotecan in platinum-resistant disease [98]. These contrasting results underline the need for prospective evaluation of individual regimens rather than inference from shared marine origin.

(5) Experimentally anchored computational discovery

Artificial intelligence can help generate hypotheses in natural product discovery, but predictions still require experimental testing. Chemical language models trained in low-data settings have been used to explore bacterial, plant, and fungal chemical space, offering a way to propose candidates when large training sets are unavailable [105]. Integration with biosynthetic annotation and measured activity may improve prioritization; generated structures or docking scores alone do not establish a target, selectivity, or anti-ovarian-cancer efficacy [11,96].

A practical research agenda starts by defining the decision that each experiment will inform: confirming a target, identifying a responsive ovarian subtype, demonstrating exposure-linked efficacy, improving tolerability, or establishing a sustainable supply route. Figure 7 integrates these requirements into a proposed development framework. It is a guide for future studies, not a claim that all reviewed candidates have completed every step.

6. Conclusions

Marine natural products offer diverse scaffolds and several well-characterized mechanisms relevant to ovarian cancer. The reviewed literature documents effects on proliferation, apoptosis, invasion, angiogenesis, and drug response, although direct target evidence is available for only part of the inventory. The strongest examples are compound-specific and include defined tubulin interactions, functional pathway perturbation, and selected demonstrations of animal efficacy.

Translation remains limited by weak links between cellular potency, causal mechanism, relevant disease models, and achievable exposure. Marine provenance, structural complexity, and changes in multiple signaling markers cannot substitute for target engagement, selectivity, or clinical evidence. Likewise, activity in a resistant cell line should not be described as restored sensitivity to the original treatment without combination data.

The next experiment should address the principal uncertainty for each lead. Priorities include histotype-appropriate models, orthogonal target validation, exposure-linked efficacy and toxicity, and reproducible production. Combination and delivery strategies require matched controls to determine whether they genuinely improve efficacy or safety.

An evidence-guided approach can turn marine chemical diversity into better research probes and more credible development candidates. Clinical advancement will depend on reproducible pharmacology and a feasible therapeutic window. Both positive and negative clinical experience should inform expectations for recurrent and treatment-resistant ovarian cancer.

Author Contributions: Conceptualization, J.J. and F.K.; data curation, J.J. and D.X.; writing—original draft preparation, J.J. and Y.W.; writing—review and editing, D.X. and P.W.; visualization, S.L. and T.F.; supervision, F.K.; project administration, L.Z.; funding acquisition, F.K. and R.Z. All authors have read and agreed to the published version of the manuscript.

Funding: This research was funded by the Scientific Research Fund of Guangxi Minzu University (No. 2021KJQD09), the Guangxi Science and Technology Program (No. GK LT2600640009), and the National Natural Science Foundation of China (No. 82360699).

Institutional Review Board Statement: Not applicable.

Data Availability Statement: The data discussed in this review are reported in the cited publications. No new experimental data were generated for this review.

Acknowledgments: Kimi-K3 assisted with literature synthesis, manuscript drafting and language revision. Figures were drawn and exported using Python 3.14 and Inkscape 1.4.4. The authors are responsible for verifying the final text, citations, and figures.

Conflicts of Interest: The authors declare no conflict of interest.

References

1. Lheureux, S.; Gourley, C.; Vergote, I.; Oza, A.M. Epithelial ovarian cancer. *Lancet* **2019**, *393*, 1240–1253. [CrossRef] [PubMed]
2. Menon, U.; Gentry-Maharaj, A.; Burnell, M.; Singh, N.; Ryan, A.; Karpinskyj, C.; Carlino, G.; Taylor, J.; Massingham, S.K.; Raikou, M.; et al. Ovarian cancer population screening and mortality after long-term follow-up in the UK Collaborative Trial of Ovarian Cancer Screening (UKCTOCS): A randomised controlled trial. *Lancet* **2021**, *397*, 2182–2193. [CrossRef] [PubMed]
3. Galluzzi, L.; Senovilla, L.; Vitale, I.; Michels, J.; Martins, I.; Kepp, O.; Castedo, M.; Kroemer, G. Molecular mechanisms of cisplatin resistance. *Oncogene* **2012**, *31*, 1869–1883. [CrossRef] [PubMed]
4. Ghaboura, N. Unraveling the Hippo pathway: YAP/TAZ as central players in cancer metastasis and drug resistance. *EXCLI J.* **2025**, *24*, 612–637. [CrossRef] [PubMed]
5. Moore, K.; Colombo, N.; Scambia, G.; Kim, B.G.; Oaknin, A.; Friedlander, M.; Lisyanskaya, A.; Floquet, A.; Leary, A.; Sonke, G.S.; et al. Maintenance olaparib in patients with newly diagnosed advanced ovarian cancer. *N. Engl. J. Med.* **2018**, *379*, 2495–2505. [CrossRef] [PubMed]

6. González-Martín, A.; Pothuri, B.; Vergote, I.; DePont Christensen, R.; Graybill, W.; Mirza, M.R.; McCormick, C.; Lorusso, D.; Hoskins, P.; Freyer, G.; et al. Niraparib in patients with newly diagnosed advanced ovarian cancer. *N. Engl. J. Med.* **2019**, *381*, 2391–2402. [CrossRef] [PubMed]
7. Lord, C.J.; Ashworth, A. PARP inhibitors: Synthetic lethality in the clinic. *Science* **2017**, *355*, 1152–1158. [CrossRef] [PubMed]
8. Matulonis, U.A.; Shapira-Frommer, R.; Santin, A.D.; Lisyanskaya, A.S.; Pignata, S.; Vergote, I.; Raspagliesi, F.; Sonke, G.S.; Birrer, M.; Provencher, D.M.; et al. Antitumor activity and safety of pembrolizumab in patients with advanced recurrent ovarian cancer: Results from the phase II KEYNOTE-100 study. *Ann. Oncol.* **2019**, *30*, 1080–1087. [CrossRef] [PubMed]
9. Luo, Y.; Xia, Y.; Liu, D.; Li, X.; Li, H.; Liu, J.; Zhou, D.; Dong, Y.; Li, X.; Qian, Y.; et al. Neoadjuvant PARPi or chemotherapy in ovarian cancer informs targeting effector Treg cells for homologous-recombination-deficient tumors. *Cell* **2024**, *187*, 4905–4925.e24. [CrossRef] [PubMed]
10. Li, M.Y.; Zhang, Q.; Li, J.; Zengin, G. Food and medicine homology in cancer treatment: Traditional thoughts collide with scientific evidence. *Food Med. Homol.* **2025**, *2*, 9420120. [CrossRef]
11. Liu, Z.P.; Tang, W.S.; Wang, G.Z.; Xu, J.W.; Zhu, L.J.; Lyu, Q.Y.; Wang, W.Q.; Chen, X.; Ding, W.P. Ferulic acid inhibiting colon cancer cells at different duke's stages. *Food Med. Homol.* **2025**, *2*, 9420063. [CrossRef]
12. Wang, E.; Sorolla, M.A.; Gopal Krishnan, P.D.; Sorolla, A. From seabed to bedside: A review on promising marine anticancer compounds. *Biomolecules* **2020**, *10*, 248. [CrossRef] [PubMed]
13. Alves, C.; Diederich, M. Marine natural products as anticancer agents. *Mar. Drugs* **2021**, *19*, 447. [CrossRef] [PubMed]
14. Muttiah, B.; Abdullah, N.A.H. Natural compounds in ovarian cancer: Mechanistic insights and therapeutic potential. *Front. Pharmacol.* **2026**, *16*, 1687805. [CrossRef] [PubMed]
15. Lu, X.W.; Qin, S.; Wang, Q.; Lu, C.Y.; Li, W.J. Functional activity and mechanisms of common marine traditional chinese medicine. *Food Med. Homol.* **2025**, *2*, 9420075. [CrossRef]
16. Salvi, A.; Amrine, C.S.M.; Austin, J.R.; Kilpatrick, K.; Russo, A.; Lantvit, D.; Calderon-Gierszal, E.; Mattes, Z.; Pearce, C.J.; Grinstaff, M.W.; et al. Verticillin a causes apoptosis and reduces tumor burden in high-grade serous ovarian cancer by inducing DNA damage. *Mol. Cancer Ther.* **2020**, *19*, 89–100. [CrossRef] [PubMed]
17. Burney, I.A.; Tamimi, Y.; Abdulla, N.; Al Balushi, N.; Al Dahlali, B.; Al Bahlani, S.; Hasan, S.I.; Dobretsov, S. Marine natural products with cytotoxic properties against epithelial ovarian cancer. *J. Agric. Mar. Sci.* **2024**, *29*, 33–41. [CrossRef]
18. Pang, K.L.; Overy, D.P.; Jones, E.G.; Calado, M.d.L.; Burgaud, G.; Walker, A.K.; Johnson, J.A.; Kerr, R.G.; Cha, H.J.; Bills, G.F. 'Marine fungi' and 'marine-derived fungi' in natural product chemistry research: Toward a new consensual definition. *Fungal Biol. Rev.* **2016**, *30*, 163–175. [CrossRef]
19. Wilson, M.C.; Mori, T.; Rückert, C.; Uria, A.R.; Helf, M.J.; Takada, K.; Gernert, C.; Steffens, U.A.E.; Heycke, N.; Schmitt, S.; et al. An environmental bacterial taxon with a large and distinct metabolic repertoire. *Nature* **2014**, *506*, 58–62. [CrossRef] [PubMed]
20. Chen, Y.F.; Wang, S.Y.; Shen, H.; Yao, X.F.; Zhang, F.L.; Lai, D. The marine-derived fungal metabolite, terrein, inhibits cell proliferation and induces cell cycle arrest in human ovarian cancer cells. *Int. J. Mol. Med.* **2014**, *34*, 1591–1598. [CrossRef] [PubMed]
21. Uz Zaman, K.A.; Sarotti, A.M.; Wu, X.; DeVine, L.; Cao, S. Polyketides, diketopiperazines and an isochromanone from the marine-derived fungal strain *Fusarium graminearum* FM1010 from Hawaii. *Phytochemistry* **2022**, *198*, 113138. [CrossRef] [PubMed]
22. Ebada, S.S.; Fischer, T.; Klaßen, S.; Hamacher, A.; Roth, Y.O.; Kassack, M.U.; Roth, E.H. A new cytotoxic steroid from co-fermentation of two marine alga-derived micro-organisms. *Nat. Prod. Res.* **2014**, *28*, 1241–1245. [CrossRef] [PubMed]
23. Frank, M.; Özkaya, F.C.; Müller, W.E.G.; Hamacher, A.; Kassack, M.U.; Lin, W.; Liu, Z.; Proksch, P. Cryptic secondary metabolites from the sponge-associated fungus *Aspergillus ochraceus*. *Mar. Drugs* **2019**, *17*, 99. [CrossRef] [PubMed]
24. Frank, M.; Hartmann, R.; Plenker, M.; Mándi, A.; Kurtán, T.; Özkaya, F.C.; Müller, W.E.G.; Kassack, M.U.; Hamacher, A.; Lin, W.; et al. Brominated azaphilones from the sponge-associated fungus *Penicillium canescens* strain 4.14.6a. *J. Nat. Prod.* **2019**, *82*, 2159–2166. [CrossRef] [PubMed]
25. Choi, H.Y.; Ahn, J.H.; Kwon, H.; Yim, J.H.; Lee, D.; Choi, J.H. Citromycin isolated from the antarctic marine-derived fungi, *Sporothrix* sp., inhibits ovarian cancer cell invasion via suppression of ERK signaling. *Mar. Drugs* **2022**, *20*, 275. [CrossRef] [PubMed]
26. Yu, G.; Wu, G.; Sun, Z.; Zhang, X.; Che, Q.; Gu, Q.; Zhu, T.; Li, D.; Zhang, G. Cytotoxic Tetrahydroxanthone dimers from the mangrove-associated fungus *Aspergillus versicolor* HDN1009. *Mar. Drugs* **2018**, *16*, 335. [CrossRef] [PubMed]
27. Bo, X.; Zhao, Y.; Qin, F.; Wu, F.; Tan, M.; Ju, S.; Song, Z.; Li, W.; He, F.; Wei, Y.; et al. Cytotoxic metabolites from the mangrove endophytic fungus *Aspergillus* sp. GXNU QG1a. *Nat. Prod. Res.* **2025**, *39*, 2572–2579. [CrossRef] [PubMed]
28. Wu, G.; Qi, X.; Mo, X.; Yu, G.; Wang, Q.; Zhu, T.; Gu, Q.; Liu, M.; Li, J.; Li, D. Structure-based discovery of cytotoxic dimeric tetrahydroxanthones as potential topoisomerase I inhibitors from a marine-derived fungus. *Eur. J. Med. Chem.* **2018**, *148*, 268–278. [CrossRef] [PubMed]

29. Luo, H.; Li, B.; Li, Z.; Cutler, S.J.; Rankin, G.O.; Chen, Y.C. Chaetoglobosin K inhibits tumor angiogenesis through downregulation of vascular epithelial growth factor-binding hypoxia-inducible factor 1α. *Anti-Cancer Drugs* **2013**, *24*, 715–724. [CrossRef] [PubMed]
30. Wang, Y.; Compton, C.; Rankin, G.O.; Cutler, S.J.; Rojanasakul, Y.; Tu, Y.; Chen, Y.C. 3-Hydroxyterphenyllin, a natural fungal metabolite, induces apoptosis and S phase arrest in human ovarian carcinoma cells. *Int. J. Oncol.* **2017**, *50*, 1392–1402. [CrossRef] [PubMed]
31. Meng, L.H.; Wang, C.Y.; Mándi, A.; Li, X.M.; Hu, X.Y.; Kassack, M.U.; Kurtán, T.; Wang, B.-G. Three Diketopiperazine alkaloids with spirocyclic skeletons and one bisthiodiketopiperazine derivative from the mangrove-derived endophytic fungus *Penicillium brocae* MA-231. *Org. Lett.* **2016**, *18*, 5304–5307. [CrossRef] [PubMed]
32. Kim, M.C.; Cullum, R.; Machado, H.; Smith, A.J.; Yang, I.; Rodvold, J.J.; Fenical, W. Photopiperazines A–D, photosensitive interconverting diketopiperazines with significant and selective activity against U87 glioblastoma cells, from a rare, marine-derived actinomycete of the family Streptomycetaceae. *J. Nat. Prod.* **2019**, *82*, 2262–2267. [CrossRef] [PubMed]
33. Mullowney, M.W.; Ó hAinmhire, E.; Tanouye, U.; Burdette, J.E.; Pham, V.C.; Murphy, B.T. A pimarane diterpene and cytotoxic angucyclines from a marine-derived *Micromonospora* sp. in Vietnam's East Sea. *Mar. Drugs* **2015**, *13*, 5815–5827. [CrossRef] [PubMed]
34. Gao, X.; Lu, Y.; Xing, Y.; Ma, Y.; Lu, J.; Bao, W.; Wang, Y.; Xi, T. A novel anticancer and antifungus phenazine derivative from a marine actinomycete BM-17. *Microbiol. Res.* **2012**, *167*, 616–622. [CrossRef] [PubMed]
35. Zhou, B.; Ji, Y.Y.; Zhang, H.J.; Shen, L. Gephyyamycin and cysrabelomycin, two new angucyclinone derivatives from the *Streptomyces* sp. HN-A124. *Nat. Prod. Res.* **2021**, *35*, 2117–2122. [CrossRef] [PubMed]
36. Martin, G.D.A.; Tan, L.T.; Jensen, P.R.; Dimayuga, R.E.; Fairchild, C.R.; Raventos-Suarez, C.; Fenical, W. Marmycins A and B, cytotoxic pentacyclic C-Glycosides from a marine sediment-derived actinomycete related to the genus *Streptomyces*. *J. Nat. Prod.* **2007**, *70*, 1406–1409. [CrossRef] [PubMed]
37. Matsuo, Y.; Kanoh, K.; Yamori, T.; Kasai, H.; Katsuta, A.; Adachi, K.; Shin-ya, K.; Shizuri, Y. Urukthapelstatin A, a Novel cytotoxic substance from marine-derived *Mechercharimyces asporophorigenens* YM11-542. *J. Antibiot.* **2007**, *60*, 251–255. [CrossRef] [PubMed]
38. Medina, R.A.; Goeger, D.E.; Hills, P.; Mooberry, S.L.; Huang, N.; Romero, L.I.; Ortega-Barría, E.; Gerwick, W.H.; McPhail, K.L. Coibamide A, a potent antiproliferative cyclic depsipeptide from the panamanian marine cyanobacterium *Leptolyngbya* sp. *J. Am. Chem. Soc.* **2008**, *130*, 6324–6325. [CrossRef] [PubMed]
39. Tranter, D.; Paatero, A.O.; Kawaguchi, S.; Kazemi, S.; Serrill, J.D.; Kellosalo, J.; Vogel, W.K.; Richter, U.; Mattos, D.R.; Wan, X.; et al. Coibamide a targets Sec61 to prevent biogenesis of secretory and membrane proteins. *ACS Chem. Biol.* **2020**, *15*, 2125–2136. [CrossRef] [PubMed]
40. Marquez, B.L.; Watts, K.S.; Yokochi, A.; Roberts, M.A.; Verdier-Pinard, P.; Jimenez, J.I.; Hamel, E.; Scheuer, P.J.; Gerwick, W.H. Structure and absolute stereochemistry of hectochlorin, a potent stimulator of actin assembly. *J. Nat. Prod.* **2002**, *65*, 866–871. [CrossRef] [PubMed]
41. Ebada, S.S.; Schulz, B.; Wray, V.; Totzke, F.; Kubbutat, M.H.; Müller, W.E.; Hamacher, A.; Kassack, M.U.; Lin, W.; Proksch, P. Arthrinins A–D: Novel diterpenoids and further constituents from the sponge derived fungus *Arthrinium* sp. *Bioorg. Med. Chem.* **2011**, *19*, 4644–4651. [CrossRef] [PubMed]
42. Zöllinger, M.; Kelter, G.; Fiebig, H.H.; Lindel, T. Antitumor activity of the marine natural product dibromophakellstatin in vitro. *Bioorg. Med. Chem. Lett.* **2007**, *17*, 346–349. [CrossRef] [PubMed]
43. Charan, R.D.; McKee, T.C.; Boyd, M.R. Cytotoxic alkaloids from the marine sponge *Thorectandra* sp. *Nat. Prod. Res.* **2004**, *18*, 225–229. [CrossRef] [PubMed]
44. Harinantenaina, L.; Brodie, P.J.; Maharavo, J.; Bakary, G.; TenDyke, K.; Shen, Y.; Kingston, D.G. Antiproliferative homoscalarane sesterterpenes from two Madagascan sponges. *Bioorg. Med. Chem.* **2013**, *21*, 2912–2917. [CrossRef] [PubMed]
45. Jiao, W.H.; Xu, T.T.; Yu, H.B.; Mu, F.R.; Li, J.; Li, Y.S.; Yang, F.; Han, B.N.; Lin, H.W. Dysidaminones A–M, cytotoxic and NF-κB inhibitory sesquiterpene aminoquinones from the South China Sea sponge *Dysidea fragilis*. *RSC Adv.* **2014**, *4*, 9236–9246. [CrossRef]
46. Ahn, J.H.; Woo, J.H.; Rho, J.R.; Choi, J.H. Anticancer Activity of Gukulenin A Isolated from the marine sponge *Phorbas gukhulensis* in vitro and in vivo. *Mar. Drugs* **2019**, *17*, 126. [CrossRef] [PubMed]
47. Clement, J.A.; Li, M.; Hecht, S.M.; Kingston, D.G.I. Bioactive isomalabaricane triterpenoids from *Rhabdastrella globostellata* that stabilize the binding of DNA polymerase β to DNA. *J. Nat. Prod.* **2006**, *69*, 373–376. [CrossRef] [PubMed]
48. Sata, N.; Abinsay, H.; Yoshida, W.Y.; Horgen, F.D.; Sitachitta, N.; Kelly, M.; Scheuer, P.J. Lehualides A−D, metabolites from a hawaiian sponge of the genus *Plakortis*. *J. Nat. Prod.* **2005**, *68*, 1400–1403. [CrossRef] [PubMed]
49. Sandler, J.S.; Colin, P.L.; Kelly, M.; Fenical, W. Cytotoxic macrolides from a new species of the deep-water marine sponge *Leiodermatium*. *J. Org. Chem.* **2006**, *71*, 7245–7251. [CrossRef] [PubMed]
50. Field, J.J.; Singh, A.J.; Kanakkanthara, A.; Halafihi, T.; Northcote, P.T.; Miller, J.H. Microtubule-stabilizing activity of zampanolide, a potent macrolide isolated from the tongan marine sponge *Cacospongia mycofijiensis*. *J. Med. Chem.* **2009**, *52*, 7328–7332. [CrossRef] [PubMed]

51. Burres, N.S.; Clement, J.J. Antitumor activity and mechanism of action of the novel marine natural products mycalamide-A and -B and onnamide. *Cancer Res.* **1989**, *49*, 2935–2940. [PubMed]
52. Schmidt, E.W.; Raventos-Suarez, C.; Bifano, M.; Menendez, A.T.; Fairchild, C.R.; Faulkner, D.J. Scleritodermin A, a cytotoxic cyclic peptide from the lithistid sponge *Scleritoderma nodosum*. *J. Nat. Prod.* **2004**, *67*, 475–478. [CrossRef] [PubMed]
53. Mokhlesi, A.; Stuhldreier, F.; Wex, K.W.; Berscheid, A.; Hartmann, R.; Rehberg, N.; Sureechatchaiyan, P.; Chaidir, C.; Kassack, M.U.; Kalscheuer, R.; et al. Cyclic cystine-bridged peptides from the marine sponge *Clathria basilana* induce apoptosis in tumor cells and depolarize the bacterial cytoplasmic membrane. *J. Nat. Prod.* **2017**, *80*, 2941–2952. [CrossRef] [PubMed]
54. Tabudravu, J.N.; Jaspars, M.; Morris, L.A.; Kettenes-van den Bosch, J.J.; Smith, N. Two distinct conformers of the cyclic heptapeptide phakellistatin 2 isolated from the fijian marine sponge *Stylotella aurantium*. *J. Org. Chem.* **2002**, *67*, 8593–8601. [CrossRef] [PubMed]
55. Fukuoka, K.; Yamagishi, T.; Ichihara, T.; Nakaike, S.; Iguchi, K.; Yamada, Y.; Fukumoto, H.; Yoneda, T.; Samata, K.; Ikeya, H.; et al. Mechanism of action of aragusterol a (YTA0040), a potent anti-tumor marine steroid targeting the G1 phase of the cell cycle. *Int. J. Cancer* **2000**, *88*, 810–819. [CrossRef] [PubMed]
56. Mooberry, S.L.; Tien, G.; Hernandez, A.H.; Plubrukarn, A.; Davidson, B.S. Laulimalide and isolaulimalide, new paclitaxel-like microtubule-stabilizing agents. *Cancer Res.* **1999**, *59*, 653–660. [PubMed]
57. Gaitanos, T.N.; Buey, R.M.; Díaz, J.F.; Northcote, P.T.; Teesdale-Spittle, P.; Andreu, J.M.; Miller, J.H. Peloruside a does not bind to the taxoid site on β-tubulin and retains its activity in multidrug-resistant cell lines. *Cancer Res.* **2004**, *64*, 5063–5067. [CrossRef] [PubMed]
58. Huang, G.S.; Lopez-Barcons, L.; Freeze, B.S.; Smith, A.B.; Goldberg, G.L.; Horwitz, S.B.; McDaid, H.M. Potentiation of taxol efficacy by discodermolide in ovarian carcinoma xenograft-bearing mice. *Clin. Cancer Res.* **2006**, *12*, 298–304. [CrossRef] [PubMed]
59. Martello, L.A.; McDaid, H.M.; Regl, D.L.; Yang, C.P.; Meng, D.; Pettus, T.R.; Kaufman, M.D.; Arimoto, H.; Danishefsky, S.J.; Smith, A.B.; et al. Taxol and discodermolide represent a synergistic drug combination in human carcinoma cell lines. *Clin. Cancer Res.* **2000**, *6*, 1978–1987. Available online: https://pubmed.ncbi.nlm.nih.gov/10815923/ (accessed on 5 November 2026). [PubMed]
60. Esposito, G.; Teta, R.; Miceli, R.; Ceccarelli, L.; Della Sala, G.; Camerlingo, R.; Irollo, E.; Mangoni, A.; Pirozzi, G.; Costantino, V. Isolation and assessment of the in vitro anti-tumor activity of smenothiazole A and B, chlorinated thiazole-containing peptide/polyketides from the caribbean sponge, *Smenospongia aurea*. *Mar. Drugs* **2015**, *13*, 444–459. [CrossRef] [PubMed]
61. Lane, A.L.; Mular, L.; Drenkard, E.J.; Shearer, T.L.; Engel, S.; Fredericq, S.; Fairchild, C.R.; Prudhomme, J.; Le Roch, K.; Hay, M.E.; et al. Ecological leads for natural product discovery: Novel sesquiterpene hydroquinones from the red macroalga *Peyssonnelia* sp. *Tetrahedron* **2010**, *66*, 455–461. [CrossRef] [PubMed]
62. Lin, A.S.; Engel, S.; Smith, B.A.; Fairchild, C.R.; Aalbersberg, W.; Hay, M.E.; Kubanek, J. Structure and biological evaluation of novel cytotoxic sterol glycosides from the marine red alga *Peyssonnelia* sp. *Bioorg. Med. Chem.* **2010**, *18*, 8264–8269. [CrossRef] [PubMed]
63. Ahn, J.H.; Yang, Y.I.; Lee, K.T.; Choi, J.H. Dieckol, isolated from the edible brown algae Ecklonia cava, induces apoptosis of ovarian cancer cells and inhibits tumor xenograft growth. *J. Cancer Res. Clin. Oncol.* **2015**, *141*, 255–268. [CrossRef] [PubMed]
64. Sahm, B.D.B.; Florêncio, K.G.D.; Pinto, F.C.L.; Maia, A.I.V.; Rocha, C.A.M.; Jimenez, P.C.; Pessoa, O.D.L.; Lotufo, T.M.C.; Costa-Lotufo, L.V.; Wilke, D.V. Anticancer potential of piericidin A1 and derivatives isolated from *Streptomyces* sp. associated with *Palythoa variabilis* from Brazilian reefs. *Chem. Biodivers.* **2026**, *23*, e03815. [CrossRef] [PubMed]
65. Kim, M.C.; Winter, J.M.; Cullum, R.; Li, Z.; Fenical, W. Complementary genomic, bioinformatics, and chemical approaches facilitate the absolute structure assignment of ionostatin, a linear polyketide from a rare marine-derived actinomycete. *ACS Chem. Biol.* **2020**, *15*, 2507–2515. [CrossRef] [PubMed]
66. Mullowney, M.; Ó hAinmhire, E.; Shaikh, A.; Wei, X.; Tanouye, U.; Santarsiero, B.; Burdette, J.; Murphy, B. Diazaquinomycins E–G, novel diaza-anthracene analogs from a marine-derived *Streptomyces* sp. *Mar. Drugs* **2014**, *12*, 3574–3586. [CrossRef] [PubMed]
67. Madiraju, C.; Edler, M.C.; Hamel, E.; Raccor, B.S.; Balachandran, R.; Zhu, G.; Giuliano, K.A.; Vogt, A.; Shin, Y.; Fournier, J.-H.; et al. Tubulin assembly, taxoid site binding, and cellular effects of the microtubule-stabilizing agent dictyostatin. *Biochemistry* **2005**, *44*, 15053–15063. [CrossRef] [PubMed]
68. Facompré, M.; Tardy, C.; Bal-Mahieu, C.; Colson, P.; Perez, C.; Manzanares, I.; Cuevas, C.; Bailly, C. Lamellarin D: A novel potent inhibitor of topoisomerase I. *Cancer Res.* **2003**, *63*, 7392–7399. [PubMed]
69. Miyake, R.; Yamanaka, S.; Matsubara, S.; Mabuchi, S. preclinical activity of plitidepsin against clear cell carcinoma of the ovary. *Anticancer. Res.* **2021**, *41*, 4277–4285. [CrossRef] [PubMed]
70. Li, D.; Williams, J.I.; Pietras, R.J. Squalamine and cisplatin block angiogenesis and growth of human ovarian cancer cells with or without HER-2 gene overexpression. *Oncogene* **2002**, *21*, 2805–2814. [CrossRef] [PubMed]
71. Jung, J.H.; Sim, C.J.; Lee, C.O. Cytotoxic compounds from a two-sponge association. *J. Nat. Prod.* **1995**, *58*, 1722–1726. [CrossRef] [PubMed]
72. Zaman, K.A.U.; Wu, X.; Sarotti, A.M.; Cao, S. New and bioactive polyketides from Hawaiian marine-derived fungus *Trichoderma* sp. FM652. *Nat. Prod. Res.* **2022**, *36*, 5984–5990. [CrossRef] [PubMed]

73. Morgan, R.J.; Leong, L.; Chow, W.; Gandara, D.; Frankel, P.; Garcia, A.; Lenz, H.-J.; Doroshow, J.H. Phase II trial of bryostatin-1 in combination with cisplatin in patients with recurrent or persistent epithelial ovarian cancer: A California cancer consortium study. *Investig. New Drugs* **2012**, *30*, 723–728. [CrossRef] [PubMed]
74. Malfetano, J.H.; Blessing, J.A.; Jacobs, A.J. A Phase II trial of Didemnin B (NSC #335319) in patients with previously treated epithelial ovarian cancer a Gynecologic Oncology Group study. *Am. J. Clin. Oncol.* **1993**, *16*, 47–49. [CrossRef] [PubMed]
75. Huang, X.C.; Xiao, X.; Zhang, Y.K.; Talele, T.; Salim, A.; Chen, Z.S.; Capon, R. Lamellarin O, a pyrrole alkaloid from an australian marine sponge, *Ianthella* sp., reverses BCRP mediated drug resistance in cancer cells. *Mar. Drugs* **2014**, *12*, 3818–3837. [CrossRef] [PubMed]
76. Liu, S.; Yang, J.; Peng, X.; Li, J.; Zhu, C. the natural product fucoidan inhibits proliferation and induces apoptosis of human ovarian cancer cells: Focus on the PI3K/Akt signaling pathway. *Cancer Manag. Res.* **2020**, *12*, 6195–6207. [CrossRef] [PubMed]
77. Monk, B.J.; Herzog, T.J.; Kaye, S.B.; Krasner, C.N.; Vermorken, J.B.; Muggia, F.M.; Pujade-Lauraine, E.; Lisyanskaya, A.S.; Makhson, A.N.; Rolski, J.; et al. Trabectedin plus pegylated liposomal doxorubicin in recurrent ovarian cancer. *J. Clin. Oncol.* **2010**, *28*, 3107–3114. [CrossRef] [PubMed]
78. Machado, F.P.; Rodrigues, I.C.; Gales, L.; Pereira, J.A.; Costa, P.M.; Dethoup, T.; Mistry, S.; Silva, A.M.S.; Vasconcelos, V.; Kijjoa, A. New alkylpyridinium anthraquinone, isocoumarin, C-glucosyl resorcinol derivative and prenylated pyranoxanthones from the culture of a marine sponge-associated fungus, *Aspergillus stellatus* KUFA 2017. *Mar. Drugs* **2022**, *20*, 672. [CrossRef] [PubMed]
79. Kaweesa, E.N.; Bazioli, J.M.; Pierre, H.C.; Lantvit, D.D.; Kulp, S.K.; Hill, K.L.; Phelps, M.A.; Coss, C.C.; Fuchs, J.R.; Pearce, C.J.; et al. Exploration of verticillins in high-grade serous ovarian cancer and evaluation of multiple formulations in preclinical in vitro and in vivo models. *Mol. Pharm.* **2023**, *20*, 3049–3059. [CrossRef] [PubMed]
80. Udwary, D.W.; Zeigler, L.; Asolkar, R.N.; Singan, V.; Lapidus, A.; Fenical, W.; Jensen, P.R.; Moore, B.S. Genome sequencing reveals complex secondary metabolome in the marine actinomycete Salinispora tropica. *Proc. Natl. Acad. Sci. USA* **2007**, *104*, 10376–10381. [CrossRef] [PubMed]
81. Sabido, E.M.; Tenebro, C.P.; Trono, D.J.V.L.; Vicera, C.V.B.; Leonida, S.F.L.; Maybay, J.J.W.B.; Reyes-Salarda, R.; Amago, D.S.; Aguadera, A.M.V.; Octaviano, M.C.; et al. Insights into the variation in bioactivities of closely related *Streptomyces* strains from marine sediments of the Visayan Sea against ESKAPE and ovarian cancer. *Mar. Drugs* **2021**, *19*, 441. [CrossRef] [PubMed]
82. Zhao, S.; Feng, R.; Gu, Y.; Han, L.; Cong, X.; Liu, Y.; Liu, S.; Shen, Q.; Huo, L.; Yan, F. Heterologous expression facilitates the discovery and characterization of marine microbial natural products. *Eng. Microbiol.* **2024**, *4*, 100137. [CrossRef] [PubMed]
83. Mehbub, M.; Lei, J.; Franco, C.; Zhang, W. Marine sponge derived natural products between 2001 and 2010: Trends and opportunities for discovery of bioactives. *Mar. Drugs* **2014**, *12*, 4539–4577. [CrossRef] [PubMed]
84. Field, J.J.; Pera, B.; Calvo, E.; Canales, A.; Zurwerra, D.; Trigili, C.; Rodríguez-Salarichs, J.; Matesanz, R.; Kanakkanthara, A.; Wakefield, S.J.; et al. Zampanolide, a potent new microtubule-stabilizing agent, covalently reacts with the taxane luminal site in tubulin α, β-heterodimers and microtubules. *Chem. Biol.* **2012**, *19*, 686–698. [CrossRef] [PubMed]
85. Prota, A.E.; Bargsten, K.; Northcote, P.T.; Marsh, M.; Altmann, K.; Miller, J.H.; Díaz, J.F.; Steinmetz, M.O. Structural basis of microtubule stabilization by laulimalide and peloruside A. *Angew. Chem. Int. Ed.* **2014**, *53*, 1621–1625. [CrossRef] [PubMed]
86. Mondal, A.; Bose, S.; Banerjee, S.; Patra, J.K.; Malik, J.; Mandal, S.K.; Kilpatrick, K.L.; Das, G.; Kerry, R.G.; Fimognari, C.; et al. Marine cyanobacteria and microalgae metabolites—A rich source of potential anticancer drugs. *Mar. Drugs* **2020**, *18*, 476. [CrossRef] [PubMed]
87. Kim, E.H.; Lee, H.H.; Choi, J.H.; Ahn, J.H. Phlorotannins from Ecklonia cava regulate dual signaling pathways, IL-17RA/Act1 and ERK1/2, to suppress ovarian cancer progression and tumor-associated macrophage activation. *Mar. Drugs* **2026**, *24*, 12. [CrossRef] [PubMed]
88. Domcke, S.; Sinha, R.; Levine, D.A.; Sander, C.; Schultz, N. Evaluating cell lines as tumour models by comparison of genomic profiles. *Nat. Commun.* **2013**, *4*, 2126. [CrossRef] [PubMed]
89. Nieto, M.A.; Huang, R.Y.J.; Jackson, R.A.; Thiery, J.P. EMT: 2016. *Cell* **2016**, *166*, 21–45. [CrossRef] [PubMed]
90. Burger, R.A.; Brady, M.F.; Bookman, M.A.; Fleming, G.F.; Monk, B.J.; Huang, H.; Mannel, R.S.; Homesley, H.D.; Fowler, J.; Greer, B.E.; et al. Incorporation of bevacizumab in the primary treatment of ovarian cancer. *N. Engl. J. Med.* **2011**, *365*, 2473–2483. [CrossRef] [PubMed]
91. Lv, C.; Ren, C.; Yu, Y.; Yin, H.; Huang, C.; Yang, G.; Hong, Y. Wentilactone A reverses the NF-κB/ECM1 signaling-induced cisplatin resistance through inhibition of IKK/IκB in ovarian cancer cells. *Nutrients* **2022**, *14*, 3790. [CrossRef] [PubMed]
92. Wang, X.; Miao, Y.H.; Zhao, X.M.; Liu, X.; Hu, Y.W.; Deng, D.W. Perspectives on Organ-on-a-Chip Technology for Natural Products Evaluation. *Food Med. Homol.* **2024**, *1*, 9420013. [CrossRef]
93. Kim, J.H.; Rho, J.R.; Choi, J.H. Marine sponge-derived gukulenin A sensitizes ovarian cancer cells to PARP inhibition via ferroptosis induction. *Mar. Drugs* **2025**, *23*, 138. [CrossRef] [PubMed]
94. Wang, Y.; Mao, Y.; Liu, H.; Huang, Y.; Xu, R. Fucoxanthin from *Laminaria japonica* targeting PANoptosis and ferroptosis pathways: Insights into its therapeutic potential against ovarian cancer. *Mar. Drugs* **2025**, *23*, 123. [CrossRef] [PubMed]

95. Tardy, C.; Facompré, M.; Laine, W.; Baldeyrou, B.; García-Gravalos, D.; Francesch, A.; Mateo, C.; Pastor, A.; Jiménez, J.A.; Manzanares, I.; et al. Topoisomerase I-mediated DNA cleavage as a guide to the development of antitumor agents derived from the marine alkaloid lamellarin D: Triester derivatives incorporating amino acid residues. *Bioorg. Med. Chem.* **2004**, *12*, 1697–1712. [CrossRef] [PubMed]
96. Blin, K.; Shaw, S.; Augustijn, H.E.; Reitz, Z.L.; Biermann, F.; Alanjary, M.; Fetter, A.; Terlouw, B.R.; Metcalf, W.W.; Helfrich, E.J.N.; et al. AntiSMASH 7.0: New and improved predictions for detection, regulation, chemical structures and visualisation. *Nucleic Acids Res.* **2023**, *51*, W46–W50. [CrossRef] [PubMed]
97. Paz, A.L.; Borghaei, H.; Liu, S.V.; Peters, S.; Herbst, R.S.; Stencel, K.; Majem, M.; Şendur, M.A.N.; Czyżewicz, G.; Bernabé Caro, R.; et al. Efficacy and safety of first-line maintenance therapy with lurbinectedin plus atezolizumab in extensive-stage small-cell lung cancer (IMforte): A randomised, multicentre, open-label, phase 3 trial. *Lancet* **2025**, *405*, 2129–2143. [CrossRef] [PubMed]
98. Gaillard, S.; Oaknin, A.; Ray-Coquard, I.; Vergote, I.; Scambia, G.; Colombo, N.; Fernandez, C.; Alfaro, V.; Kahatt, C.; Nieto, A.; et al. Lurbinectedin versus pegylated liposomal doxorubicin or topotecan in patients with platinum-resistant ovarian cancer: A multicenter, randomized, controlled, open-label phase 3 study (CORAIL). *Gynecol. Oncol.* **2021**, *163*, 237–245. [CrossRef] [PubMed]
99. Spicka, I.; Ocio, E.M.; Oakervee, H.E.; Greil, R.; Banh, R.H.; Huang, S.-Y.; D'Rozario, J.M.; Dimopoulos, M.A.; Martínez, S.; Extremera, S.; et al. Randomized phase III study (ADMYRE) of plitidepsin in combination with dexamethasone vs. dexamethasone alone in patients with relapsed/refractory multiple myeloma. *Ann. Hematol.* **2019**, *98*, 2139–2150. [CrossRef] [PubMed]
100. Bhargava, P.; Marshall, J.L.; Dahut, W.; Rizvi, N.; Trocky, N.; Williams, J.I.; Hait, H.; Song, S.; Holroyd, K.J.; Hawkins, M.J. A phase I and pharmacokinetic study of squalamine, a novel antiangiogenic agent, in patients with advanced cancers. *Clin. Cancer Res.* **2001**, *7*, 3912–3919. [PubMed]
101. Moore, K.N.; Angelergues, A.; Konecny, G.E.; García, Y.; Banerjee, S.; Lorusso, D.; Lee, J.-Y.; Moroney, J.W.; Colombo, N.; Roszak, A.; et al. Mirvetuximab soravtansine in FRα-positive, platinum-resistant ovarian cancer. *N. Engl. J. Med.* **2023**, *389*, 2162–2174. [CrossRef] [PubMed]
102. Armstrong, D.K.; Bundy, B.; Wenzel, L.; Huang, H.Q.; Baergen, R.; Lele, S.; Copeland, L.J.; Walker, J.L.; Burger, R.A. Intraperitoneal cisplatin and paclitaxel in ovarian cancer. *N. Engl. J. Med.* **2006**, *354*, 34–43. [CrossRef] [PubMed]
103. Paoli, L.; Ruscheweyh, H.J.; Forneris, C.C.; Hubrich, F.; Kautsar, S.; Bhushan, A.; Lotti, A.; Clayssen, Q.; Salazar, G.; Milanese, A.; et al. Biosynthetic potential of the global ocean microbiome. *Nature* **2022**, *607*, 111–118. [CrossRef] [PubMed]
104. Wilhelm, S.; Tavares, A.J.; Dai, Q.; Ohta, S.; Audet, J.; Dvorak, H.F.; Chan, W.C.W. Analysis of nanoparticle delivery to tumours. *Nat. Rev. Mater.* **2016**, *1*, 16014. [CrossRef]
105. Skinnider, M.A.; Stacey, R.G.; Wishart, D.S.; Foster, L.J. Chemical language models enable navigation in sparsely populated chemical space. *Nat. Mach. Intell.* **2021**, *3*, 759–770. [CrossRef]

Disclaimer/Publisher's Note: The statements, opinions and data contained in all publications are solely those of the individual author(s) and contributor(s) and not of MDPI and/or the editor(s). MDPI and/or the editor(s) disclaim responsibility for any injury to people or property resulting from any ideas, methods, instructions or products referred to in the content.